VALIDATION OF THE WATER PRODUCTIVITY UNDER SOIL MOISTURE STRESS FOR DIFFERENT AGRO-ECOLOGICAL ZONES OF RWANDA

BELLE ANGE NIYONSHUTI
July, 2021

SUPERVISORS:
Dr. B.H.P. Maathuis
Dr.ir. C. van der Tol

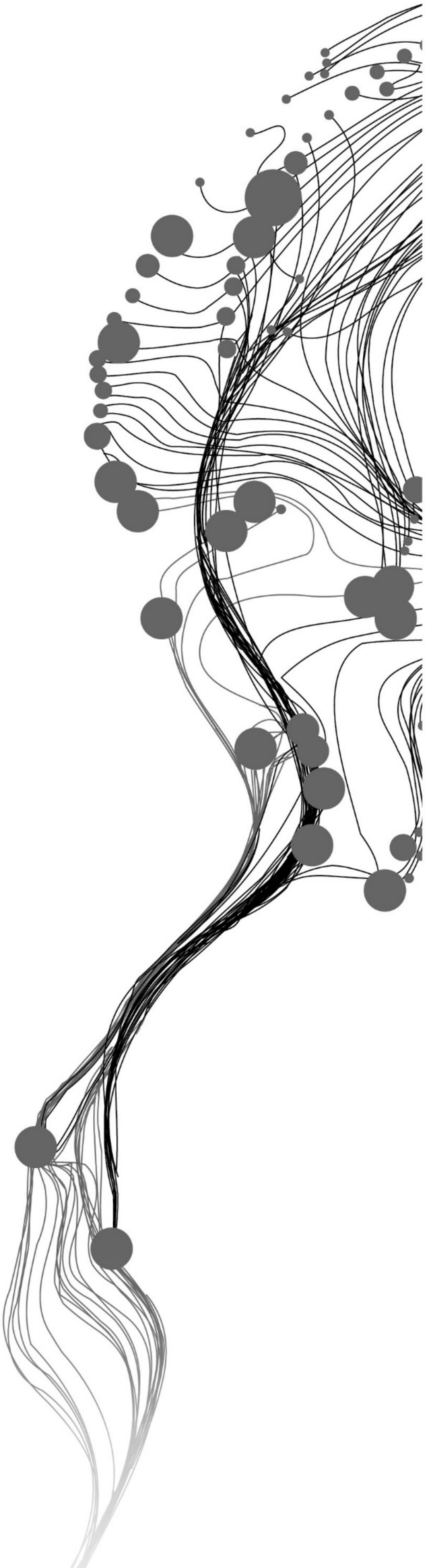

VALIDATION OF THE WATER PRODUCTIVITY UNDER SOIL MOISTURE STRESS FOR DIFFERENT AGRO-ECOLOGICAL ZONES OF RWANDA.

BELLE ANGE NIYONSUTI
Enschede, The Netherlands, July, 2021.

Thesis submitted to the Faculty of Geo-Information Science and Earth Observation of the University of Twente in partial fulfilment of the requirements for the degree of Master of Science in Geo-information Science and Earth Observation.
Specialization: Water Resources and Environmental Management

SUPERVISORS:
Dr. B.H.P. Maathuis
Dr.ir. C. van der Tol

THESIS ASSESSMENT BOARD:
Dr. Ing. T.H.M. Rientjes (Chair)
Dr. Ir. A. Vrieling (External Examiner, UT-ITC-NRS)

ABSTRACT

Soil moisture availability is one of the most important parameters governing biomass production and actual evapotranspiration (ETa), key parameters used to determine the Water Productivity provided by FAO-WaPOR. The triangle method is one of approaches incorporating soil moisture availability as one of the factors which could reduce the ETa due to environmental stress. This approach is based on correlating Normalized Difference Vegetation Index (NDVI) and Land Surface Temperature (LST) retrieved from remote sensing to the ground measured soil moisture. For this study, no in-situ soil moisture was available, hence observed soil moisture from SMOS level 2 was used. The triangle method was investigated on four landcover types (Akagera savanna, Nyungwe forest, tea and eucalyptus) located in three distinctive major agro-ecological zones of Rwanda.

The triangle method was best applied for the sample areas especially for Akagera savanna as the three most important properties of the triangle method were well observed (cold edge, peak of the triangle and warm edge). On the other hand, the methodology was not applicable to Nyungwe forest because there is no edge to be found (no warm or cold edge in the scatter plot). There is no limiting factor related to soil moisture as this is a mountain rain forest, hence it was not considered for further analysis. The results of the triangle method indicated that all sample areas are under soil moisture stress conditions for the period investigated especially Akagera savanna with soil moisture stress factor of 0.15 .

Validation of FAO-WaPOR ETIa was done by investigating the application of the triangle method for different landcover types in order to evaluate this aspect of FAO-WAPOR ETIa methodology and by comparing FAO-WaPOR ETIa to the ETa derived from two different methods. The first ETa was derived using Penman-Monteith method and it is based on climatological data, the second ETa was derived using DATTUTDUT model which is solely based on a LST image. The comparative analysis indicated that the three methods are comparable with slightly deviating values less than 1mm/day for all the sample areas probably due to the difference in spatial resolution. Both Penman-Monteith method and DATTUTDUT model ETa were in good agreement with the ETIa provided by FAO-WaPOR. Soil moisture stress affected FAO-WaPOR-ETIa by overestimating ETIa values especially when having lower soil moisture stress values. The highest overestimation in ETIa was found in Akagera savanna area which has the lowest soil moisture stress value. Therefore, the sensitivity of ETIa to stress is very high when having lower soil moisture stress values.

FAO-WaPOR does not provide some of the actual data (LST, NDVI and soil moisture stress factor) used to produce their ETIa product, therefore more detailed assessment on the evaluation of the triangle method input parameters in the aspect of FAO-WaPOR ETIa methodology was not possible. To accurately assess FAO-WaPOR ETIa product, further study on these parameters is recommended .

The output of this study is essential to FAO-WaPOR, as it could provide them useful information on how good or uncertain their products are.

Keywords: Triangle method, LST, NDVI, soil moisture stress, DATTUTDUT model, ETIa, Water Productivity, FAO-WaPOR, Penman-Monteith method.

ACKNOWLEDGEMENTS

First and foremost, I thank God for being with me throughout my studies. I would like to thank the Dutch government through NUFFIC scholarship program for this great opportunity to study at the University of Twente, ITC Faculty.

Sincere thanks to my supervisors: Ben Maathuis, Thank you for believing in me and providing the needed support. Thank you for always making time to answer my questions, making sure I was on the right track. Thank you for always being available when I needed help. Thank you for your commitment and critical comments on my research thesis.

To Christiann van der Tol, thank you for your suggestions and valuable support. Your advice and suggestions were helpful for the completion of this thesis.

I would like to thank the University of Twente through its Faculty of Geoinformation Science and Earth Observation and the Department of Water Resources especially in the WREM department for providing me both theoretical and practical skills and knowledge on remote sensing that I needed in the completion of my thesis and for my future professional life.

Special thanks to my family for their encouragement and moral support throughout my studies. To my classmates and friends met in the Netherlands, thanks for the wonderful moments we shared for the last 2 years.

TABLE OF CONTENTS

LIST OF FIGURES

LIST OF TABLES

ACRONYMS AND ABBREVIAIONS

AEZs	Agroecological zones
WP	Water Productivity
ETa	Actual evapotranspiration
ETIa	Actual evapotranspiration and interception
ETo	Reference evapotranspiration
WaPOR	Water Productivity Open-access portal of Remotely-sensed data
ILWIS	Integrated land and water information system
FAO (UN)	Food and Agriculture Organization of the United Nations
R2	Coefficient of Determination
TM	Triangle method
Kc	Crop coefficient
Ksf	Tenacity factor
Se	Relative soil moisture content
Sm	Soil moisture stress factor
SM	Soil moisture
NDVI	Normal Difference Vegetation Index
LST	Land Surface Temperature
RMSE	Roots mean square error
PM	Penman-Monteith
SMOS	Soil Moisture and Ocean Salinity
ECMWF	European Centre for Medium-Range Weather Forecasts
CDS	Climate Data Store
DATTUTDUT	Deriving Atmosphere Turbulent Transport Useful To Dummies Using Temperature

1. INTRODUCTION

1.1. Background

Water, a scarce natural resource with limited annual availability in some parts of the world, is an essential resource for agricultural production and food security (FAO, 2016a). The world's population is estimated to increase from 7.7 billion in 2019 to reach 8.5 billion in 2030, 9.7 billion in 2050, and 10.9 billion in 2100 (Prospects, 2020). Due to population growth in combination with economic growth, there is a huge demand for food with limited water resources. Water demand for agriculture is found to be the main driver for pressure on water use in many countries. Agriculture is both a cause and a victim of water scarcity (FAO, 2016b).

Rwanda is affected by climate change like other countries around the world. Hence, there is increasing competition for water resources and putting pressure on the country's water resources. The fastest increase in the Rwandan population requires increased food production, yet fewer water resources are available for agriculture. Available data shows that Rwanda is a water scarce country (African Water Facility, 2016). With a per capita freshwater availability of less than 1000 m^3 which is about a quarter of Africa's average of 4000 m^3 (African Water Facility, 2016). Thus affecting the agriculture sector in Rwanda which is not only crucial for Rwanda's growth and reduction of poverty but also economic growth.

The agriculture sector accounts for 70% of water demand in Rwanda which is the largest as compared to other sectors (Government of Rwanda (NISR), 2019). One of the major challenges for the coming years for Rwanda is to provide a safe food supply for future generations given that some regions of the country are still malnourished, especially the Eastern and Western regions. Therefore, improving agricultural productivity, while using available water resources more efficiently, is an important requirement for farmers to increase food supplies on a sustainable basis (FAO, 2017b).

Water productivity (WP) is expressed as "crop production per unit volume of water use", thus the total biomass produced divided by the actual volume of water consumed by the plant (Mali, 2016). This relationship is applied on agriculture, crop or livestock, forestry, fisheries and more. The WP is found through a combination of land use, biomass production, Interception, and Evapotranspiration (ET) data. The water productivity information can be derived based on for example WaPOR (FAO's Water Productivity open-access portal), MODIS, and Landsat.

WaPOR is an open portal launched by the Food and Agriculture Organization of the United Nations (FAO-UN) on April 20th 2017. The portal provides open access to remotely sensed datasets that enable monitoring of land and water productivity across Africa and the Near East. WaPOR's mission is to focus on stakeholders from local farmers to decision makers with an ambition to develop solutions to sustainably increase agricultural land and water production (FAO, 2017a). WP can be estimated from remote sensing derived products, ET and biomass. ET is the critical component of WP measurement that has to be accurately measured.

The triangle method (TM) introduced by Price (1990), is one of the methods used by FAO-WaPOR in their ETIa methodology to get additional information that are optimum on limiting the ET from the plant. TM is an approach which incorporates soil moisture availability as one of the factors which could reduce the ET due to environmental stress.

Soil moisture availability is one of the most important parameters governing biomass production and ETa (FAO, 2018a). In the case of soil moisture stress, the productivity is affected. Thus, the assessment of soil moisture conditions is relevant and important information related to the decrease in agricultural yield and water productivity (Jing & Li, 2014).

Many studies around the world have validated the Water Productivity using some models to ensure the quality of remote sensing products before they can be further used for decision making. Some researchers prefer to use the Soil & Water Assessment Tool (SWAT or SWAT +) (Querner, Herder, Fissahaye, & Froebrich, 2014; Vaghefi, Abbaspour, Faramarzi, Srinivasan, & Arnold, 2017) and others use the AquaCrop model (Foster et al., 2017; Jin et al., 2018; Silva et al., 2018).

In Rwanda, few studies have been conducted on water productivity only based on a combination of land uses and others based on the economic terms expressed in Rwandan franc per cubic millimeter (Rwf/m^3) (Government of Rwanda (NISR), 2019). No study was conducted on the validation of the Water Productivity. This study aims to evaluate the use of the triangle method for different agro-ecological zones of Rwanda and to determine how it affects ETa, a key parameter used to determine the Water Productivity provided by FAO-WaPOR.

1.2. Problem statement

As described above, WaPOR (FAO, 2020a) is an open portal launched by the Food and Agriculture Organization of the United Nations (FAO-UN) on April 20th 2017. The portal was launched to monitor Land and Water Productivity (WP) by providing open access to remotely sensed datasets across Africa and the Near East. The derived datasets cover the period from 01/01/2009 to present at temporal scales that vary from daily to dekadal, seasonal and annual (FAO, 2018b). The available remote sensing-based datasets cover different regions at three spatial levels. Level I at 250 m resolution, Level II at 100 m resolution and Level III at 30 m resolution (FAO & IHE Delft, 2019).

Rwanda is one of the African countries that are benefiting from WaPOR data components at 100 meters resolutions (level 2). Actual evapotranspiration (ETa) is the critical component of WP measurement that has to be accurately evaluated. With enough information about soil moisture availability, it is expected that one can get a better estimation of ETa. The triangle method is one of the methods used in FAO-WaPOR ETIa methodology to get a better estimation of ETIa. However, WaPOR still shows some bias in derived datasets mainly resulting from procedures used for deriving biomass and actual evapotranspiration (ETIa), key variables used for estimating the Water Productivity (FAO and IHE Delft, 2019). This requires some further validation. The validation was done by investigating the application of the triangle method and to check how it affects FAO-WaPOR ETIa and by comparing the ETIa-FAO-WaPOR with the ETa from other methods (Penman-Monteith method which uses climatological data and DATTUTDUT model which uses only a LST image.

1.3. Research objectives

1.3.1. Main objective

The main objective of this study is to evaluate the use of the triangle method for different agro-ecological zones (AEZs) of Rwanda and to determine how it affects ETa, a key parameter used to determine the Water Productivity provided by FAO-WaPOR.

1.3.2. Specific objectives:

- To investigate the application of the triangle method for different AEZs of Rwanda for deriving their relative soil moisture content and soil moisture stress factor.
- To evaluate the effect of soil moisture stress on FAO-WaPOR ETIa.
- To calculate the ETa using Penman-Monteith method and DATTUTDUT model.
- To compare the Penman-Monteith ETa and DATTUTDUT model ETa to the ETIa provided by FAO- WaPOR.

1.4. Research questions

- Which AEZs are representative of larger areas in Rwanda? And how different is their triangular shapes?
- How are relative soil moisture content and stress factor estimated using the triangle method?
- How does the soil moisture stress affect FAO-WaPOR ETIa?
- How to get ETa from Penman-Monteith method and from DATTUTDUT model?
- How does FAO-WaPOR ETIa compare with the ETa from Penman-Monteith method and DATTUTDUT model?

1.5. Novelty of the study

The triangle method is a methodology developed to estimate the surface soil moisture availability without using a land surface model like Soil Vegetation Atmosphere Transfer (SVAT) and that doesn't require the addition of surface and atmospheric information (Carlson & Petropoulos, 2019). Triangle method is classified as a thermal infrared technique for soil moisture estimation using remotely sensed data (Wang, Qu, Zhang, Hao, Dasgupta, 2007). It has been widely applied in other parts of the world like the United States (Carlson, 2007), Iran (Rahmati et al., 2015a), Brazil (Silva-Fuzzo & Rocha, 2016), and the Netherlands (Carlson & Petropoulos, 2019) demonstrating good performance in estimating soil moisture (Rahmati et al., 2015a). An advantage of this method is that it requires a smaller number of input variables and it estimates the soil moisture at a reasonably good spatial resolution. Fenta Mekonnen (2009) recommended to further explore the triangle method for different landcover types at different location. The novelty of this study is that it has never been investigated in detail for Rwanda. For this study, the triangle method will be investigated for different agroecological zones of Rwanda.

1.6. Structure of the thesis

The structure of this thesis consists of six chapters. Chapter 1 presents the introduction with a brief background and problem statement of the research topic, the objectives, questions and novelty aspect of the research. Chapter 2, Literature review provides an overview of the concepts of actual evapotranspiration and the description of the triangle method. Chapter 3 represents the description of the study areas and the data used in this study . Chapter 4 presents the research methodology explaining in details the overview of the main activities from the flowchart and the overview of the software used. Chapter 5 introduces and discusses the results. Chapter 6 introduces the conclusion, recommendation for future studies and limitation of the study.

2. LITERATURE REVIEW

2.1. Concept of actual evapotranspiration

Allen et al. (1998) define evapotranspiration (ET) as the combination of two separate processes whereby water is lost on the one hand from the soil surface by evaporation and on the other hand from the crop by transpiration. Evaporation is described as the process where liquid water is converted to water vapor (vaporization) and removed from sources such as the soil surface, wet vegetation, pavement, water bodies, while transpiration consists of the vaporization of liquid water within a plant and subsequent loss of water as vapor through leaf stomata (Zotarelli et al., 2020).

Saadi (2018) defines actual evapotranspiration (ETa) as the quantity of water that is actually removed from a surface due to the processes of transpiration and evaporation. In general, ETa of a crop represents the actual water consumption and it can be estimated with different methods, including: 1) Penman-Monteith method, 2) from atmospherically corrected surface temperature image using DATTUTDUT model and 3) from remote sensing data through FAO-WaPOR portal.

2.1.1. FAO Penman-Monteith method

FAO Penman-Monteith method is the sole standard method for the definition and computation of the reference evapotranspiration (ETo) recommended by FAO. This method is used to calculate ETo from meteorological data. Allen et al. (1998) define ETo as the evapotranspiration from the reference surface where the reference surface is hypothetical grass reference crop with an assumed height of 0.12m, a fixed surface resistance of $70sm^{-1}$ and an albedo of 0.23. According to Allen et al. (1998), the reference surface closely resembles an extensive surface of green, well-watered grass of uniform height, actively growing and completely shading the ground.

ETo is not influenced by land cover, hence for a daily ETo calculation, the FAO Penman-Monteith method requires daily air temperature, air humidity, solar radiation and wind speed data. In this study, the daily ETo calculation was done following the FAO-56 reference crop evapotranspiration equation. More details about step by step of the simplified form of the Penman Monteith equation is described in Zotarelli et al. (2014).

$$ET_0 = \frac{0.408\Delta(R_n - G) + \gamma\frac{900}{T+273}u_2(es - ea)}{\Delta + \gamma(1 + 0.34u_2)} \qquad \text{Equation 1}$$

where ETo = reference evapotranspiration rate (mm d-1), T = mean air temperature (°C), and u2 = wind speed (m s-1) at 2 m above the ground. Rn=net radiation flux (MJ m-2 d-1), G= sensible heat flux into the soil (MJ m-2d-1), es -ea = saturation vapor pressure deficit (kPa); Δ= Slope of saturation vapour pressure curve (kPa/^{0}C) and γ= Psychrometric constant (kPa/^{0}C).

The most common application to date of the Penman-Monteith-type equation for estimating evapotranspiration has been a three-step process. The three steps are 1) the determination of a reference Eto using Equation 1, 2) multiplying ETo by a crop coefficient (Kc) to obtain ETa for a particular crop or surface condition and 3) to adjust ETa under soil water stress conditions by multiplying ETa by a stress factor (Ks), which describes the effect of water stress on crop transpiration (Allen et al., 1998).

For this study, the first and second application f Penman-Monteith method were used. The Kc factor is used to aggregate the physical and physiological differences between crops and the reference definition (Allen et al., 1998) .
The following formula can be used:

$$ET_a = K_c ET_0 \qquad \text{Equation 2}$$

Where ETa is actual evapotranspiration, Eto is reference evapotranspiration and Kc is a crop coefficient

2.1.2. Description of the DATTUTDUT model

The Deriving Atmosphere Turbulent Transport Useful To Dummies Using Temperature (DATTUTDUT) model (Timmermans et al., 2015), is a very simple remote sensing-based and fully automated model which does not need any ancillary data. It only requires surface temperature observations acquired over the area of interest to estimate the daily evapotranspiration (Timmermans et al., 2015). This model assumes that LST is an important indicator for the surface status. The key input parameter for the DATTUTDUT model is a LST map from where the hottest (LSTmax) and the 0.5% of coldest pixels (LSTmin) are extracted, assuming that hot pixels are a result of very little to no evapotranspiration and cold pixels originate from a high evapotranspiration rate (Xia et al., 2016).

The DATTUTDUT approach uses the evaporative fraction concept in combination with daily net radiation (Rn) estimates to produce daily ETa values. According to Allen et al. (2007) and Timmermans et al. (2015), DATTUTDUT model estimates Rn like other energy balance models by computing the net shortwave radiation and the net longwave radiation:

$$R_n = (1-\alpha)S_d + \varepsilon_a \sigma T_a^4 - \varepsilon \sigma LST^4 \qquad \text{Equation 3}$$

where Rn is net radiation (Wm^{-2}), ε_a is the atmosphere emissivity (–) and ε is the effective (integrated soil + canopy) emissivity. The value of Sd is obtained from the Sun–Earth astronomical relationships under clear-sky conditions, α is the surface albedo, Ta is air temperature, LST is land surface temperature. In the DATTUTDUT model, values of ε and ε_a are set to be 0.96 and 0.7 respectively, air temperature (Ta) is assumed to be equal to the minimum LST identified within the area of interest.

Surface albedo is scaled with LST between extreme values of 0.05 and 0.25 based on the assumption that densely vegetated objects are likely to be darker and cooler while bare objects tend to appear brighter and hotter (Timmermans et al., 2015):

$$\alpha = 0.05 + \left(\frac{LST - LST_{min}}{LST_{max} - LST_{min}}\right) 0.2 \qquad \text{Equation 4}$$

where LSTmax is the maximum LST within the image, and LSTmin is the 0.5% lowest temperature in the area.

Soil heat flux is calculated from Rn with the coefficient c_G scaled between a minimum value of 0.05 for fully covered condition and maximum value of 0.45 for bare soil (Roerink et al., 2000; Santanello and Friedl, 2003):

$$c_G = \frac{G}{R_n} = 0.05 + \left(\frac{LST - LST_{min}}{LST_{max} - LST_{min}}\right) 0.4 \qquad \text{Equation 5}$$

Similar to α and c_G, evaporative fraction (EF) is assumed to be linearly related to LST:

$$EF = \frac{LE}{LE+H} = \frac{LE}{R_n-G} = \frac{LE}{A} = \frac{LST_{max}-LST}{LST_{max}-LST_{min}} \quad \text{Equation 6}$$

where A ($=R_n$-G) is available energy (Wm^{-2}), LE is latent heat, G is Soil heat flux, H is sensible flux, LSTmax is the maximum LST within the image, and LSTmin is the 0.5% lowest temperature in the area. LE can be calculated from A and EF, and H can be estimated as the residual to the energy balance equation. Then daytime evapotranspiration for each pixel can be calculated by available energy, A and the evaporative fraction, EF retrieved by DATTUTDUT:

$$ETa = A * EF \quad \text{Equation 7}$$

2.1.3. Application of DATTUTDUT model

DATTUTDUT has been applied in some parts of the world demonstrating a good performance to derive daily evapotranspiration. Ellsäßer et al. (2020) have successfully applied the DATTUTDUT model for predicting evapotranspiration from drone-based thermography. Their study showed that ET estimates of the simple DATTUTDUT model were in good agreement with the observations.

Brenner et al. (2018) conducted a study on estimation of evapotranspiration of temperate grassland based on high-resolution thermal and visible range imagery from unmanned aerial systems. They used both DATTUTDUT and TSEB-PT model, the results showed that DATTUTDUT model marginally outperformed TSEB-PT model.

Timmermans et al. (2015) conducted a study on utility of an Automated Thermal-Based Approach for Monitoring Evapotranspiration to present demonstrate advantages and limitations of the DATTUTDUT model. The DATTUTDUT algorithm was evaluated against published results from other methodologies to evaluate its utility for operational water use monitoring purposes. The overall trend of observed daily ET values over a growing season for two sites in Turkey reproduced reasonably well, with DATTUTDUT outperforming the SEBAL scheme where DATTUTDUT model results were in close agreement with the observation, whereas SEBAL model results slightly underestimated the daily ET. Timmermans et al. (2015) suggested that DATTUTDUT has utility in identifying relative water use and as an operational tool providing initial estimates of ET anomalies in data-poor regions.

2.1.4. Limitation of DATTUTDUT model

According to Timmermans et al. (2015), the limitation of the DATTUTDUT model is that it does not consider the effects of aerodynamic resistance on the heat exchange for a given surface air temperature difference, which can have a remarkable impact on the flux-gradient relationship . There are environmental conditions that limit the utility of the DATTUTDUT model. For example, when the region is under water stressed conditions, it is difficult to identify wet and dry pixels.

2.2. Description of the Triangle Method

Soil moisture plays an important role in agricultural water resources management as its availability is one of the most important parameters governing biomass production and evapotranspiration. Soil moisture can be estimated from remote sensing methods. One of the most widely used method is the Triangle Method (TM). Chauhan et al. (2003) classified this method as a thermal infrared technique for soil moisture estimation using remotely sensed data (Wang et al., 2007).

In general, TM is a method used to map land surface moisture from the normalized difference vegetation index (NDVI) and land surface temperature (LST). The method shows that there is a universal relationship among soil moisture, NDVI, and LST for a given region (Nichols, 2011) as shown in Figure 1. If a sufficiently large number of pixels are present and when cloud and surface water and outliers are removed, the shape of the pixel envelope in the feature space plot between NDVI and LST resembles a triangle (Carlson, 2007). A triangle appears because the range of surface radiant temperature decreases as the vegetation cover increases.
The advantage of this method is that it requires a smaller number of input variables. It estimates the surface soil moisture without using a land surface model like Soil Vegetation Atmosphere Transfer (SVAT) and it doesn't require the addition of surface and atmospheric information (Carlson & Petropoulos, 2019).

The limitation of the triangle method is that it requires a flat surface and a large number of pixels over an area with a wide range of soil wetness and fractional vegetation cover for the identification of the triangular shape in the pixel distribution (Carlson, 2007).

The relationship among the soil moisture, NDVI and LST is presented in the following regression formula:

$$SM = \sum_{i=0}^{i=n} \sum_{j=0}^{j=n} a_{ij} NDVI^{*(i)} LST^{*(j)} \quad \text{Equation 8}$$

where aij is the regression coefficient and the superscripts i and j imply the degree of the polynomials that are chosen for the regression. SM is estimated relative soil moisture content, NDVI* and LST* are scaled NDVI and scaled LST respectively.

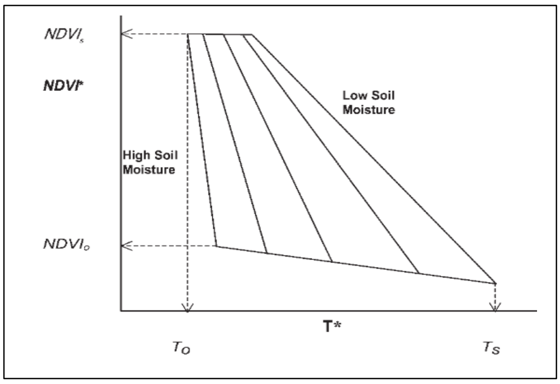

Figure 1: Universal triangle: the schematic relationship between soil moisture, scaled NDVI as NDVI* and scaled LST as T*, source (Chauhan et al., 2003).

According to Chauhan et al. (2003), there is soil moisture variation from the right to the left side of the triangle. The right side of the triangle is expected to have low soil moisture and the left side of the triangle high soil moisture. The second observation is that the surface temperature decreases as the NDVI increases which makes the slope towards the left. The third and the most important observation is on the peak of the triangle where the value of NDVI is higher but the corresponding value of surface temperature is low with a small variation. The small change of surface temperature with high NDVI indicates the wetness of the soil moisture in the vegetation.

2.2.1. Previous studies on estimation of soil moisture using the triangle method

Rahmati et al. (2015a) assessed the accuracy of the Triangle Method to calculate surface soil moisture content using MODIS satellite images with 1km resolution. They created a range of polynomial regressions from 1st to 4th orders between the ground measured soil moisture and MODIS NDVI and LST. The 4th order polynomial was shown to predict the best results of the soil moisture with the efficiency error (ER) and adjusted determination coefficient (R2adj) criteria, respectively, equal to 11.0% and 0.63 for calibration and 15.9% and 0.60 for the validation stage.

Fenta Mekonnen (2009) established three order polynomial relation. Normally, the algorithm developed using 3rd order polynomial relation is more accurate than 1st and 2nd order polynomial relation. However, from the results, the 1st and 3rd order polynomials demonstrated some errors. Hence, the 2nd order polynomial algorithm was taken to give better results with R2 greater than 0.7, and RMSE of 0.045 when comparing the simulated soil moisture with ground measured soil moisture.

Wang et al. (2007) applied the triangle method for soil moisture estimation at 1km resolution in eastern China Shandong province. The process was done by linking the ground observed soil moisture at point scale with the satellite-derived surface parameters NDVI and LST. The coefficient of determination for 55 stations was greater than 0.8, 71 stations greater than 0.7 and 82 stations were greater than 0.6. The results demonstrated the possibility of soil moisture estimation using the triangle method.

2.2.2. Application of triangle method by FAO-WaPOR

FAO-WaPOR (FAO, 2018a) uses the triangle method for deriving relative soil moisture content and soil moisture stress factor. The resulting relative soil moisture content is further used to determine the availability of water for evaporation (E) and transpiration (T) and this is calculated with a stress factor. Soil moisture stress factor (FAO, 2020b) is defined as a stress for transpiration (S_m) which is used as input for E and T to reduce evapotranspiration. S_m can be derived using the following formula (FAO, 2018a):

$$S_m = K_{sf} S_e - \frac{sin(2\pi S_e)}{2\pi} \qquad \text{Equation 9}$$

Where S_m is the soil moisture stress factor, S_e is the relative soil moisture content and K_{sf} is the tenacity factor which ranges from 1 for drought-sensitive plants to 3 for drought-insensitive (tenacious) plants. A default value of 1.5 is chosen when no crop information is available (FAO, 2018a). Pixel based soil moisture stress values range between 0 and 1, where 0 means maximum stress and 1 means no stress (FAO, 2018a). If crops are under stress conditions, ETIa is affected as it is sensitive to stress. Thus resulting in overestimation of FAO-WaPOR ETIa values. This is why they use a stress factor to reduce ETIa.

3. STUDY AREA AND DATASETS

3.1. Study areas description

According to World Bank Group (2021), Rwanda is a landlocked country in East Africa covering over 26,300 km². The country has a tropical climate, average temperature of 20 °C and 1295 mm of rainfall annually. The annual cycle consists of four seasons: two rainy seasons and two dry seasons (World Bank Group, 2021):

- a short rainy season (October - November)
- a short dry season (December - January)
- a long rainy season (February - May)
- a long dry season (June - September)

The average climatic information (temperature, rainfall and altitude) were used to divide Rwanda into 10 agroecological zones(AEZs) characterized by wide ranges in climate, topography and resulting vegetation (Bassi et al., 2020). The 10 AEZs of Rwanda are Congo-Nile Watershed Divide, Birunga, Buberuka Highlands, Impala, Imbo, Eastern Savanna and Central Bugesera, Mayaga and Peripheral Bugesera, Central Plate and Eastern Plateau. Sample areas of this study are located in three distinctive major agro-ecological zones of Rwanda.

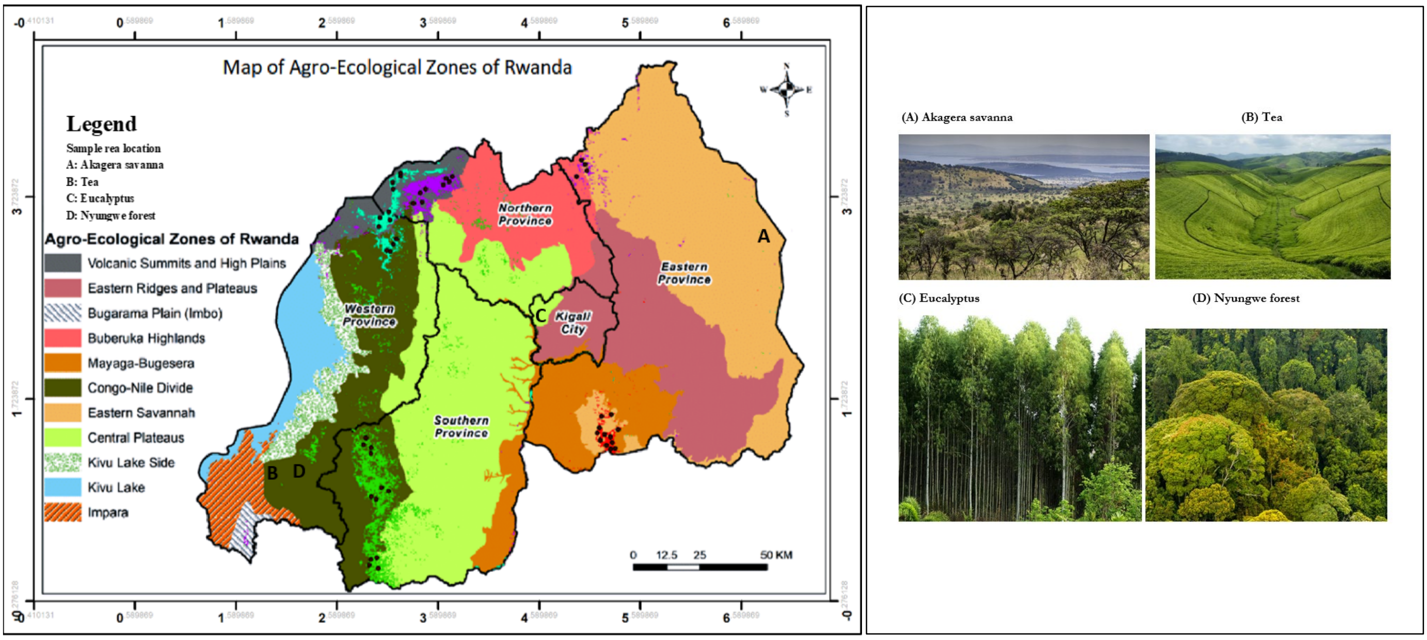

Figure 2: Map of agro-ecological zones of Rwanda, source:(Mugabowindekwe & Rwanyiziri, 2020), sample areas location and the typical land cover types.

A. Nyungwe Forest National Park and tea estate in the Congo-Nile Watershed Divide

Nyungwe forest is a moist evergreen forest in Rwanda and probably the most preserved forest in Africa (RDB, 2019). The forest is surrounded by tea plantations. Both Nyungwe forest and tea estates are located in the Congo-Nile region which has the highest elevations, steepest slopes, and the lowest average temperatures nationally (around 18.1 °C). The region has relatively fertile soils, higher precipitation and it is more attractive for farmers despite the steeply sloped terrain and soil erosion challenges (Bassi et al., 2020).

B. Akagera National Park in the Eastern Savanna and Central Bugesera

Akagera National Park is the largest protected wetland in Central Africa and the last remaining refuge for savannah-adapted species in Rwanda (RDB, 2019). It is characterized by woodland, swamp, undulating topography with occasional low mountains, and extensive grassland savanna. Akagera national park is located in the Eastern Savanna and Central Bugesera AEZ, the elevation is lower, the topography is flatter, and the climate is warmer and drier, with temperatures ranging from 21.7–22 °C (Bassi et al., 2020) and with an annual average precipitation of 750 - 850 mm (Macpherson, 2013) .

C. Eucalyptus in the Central Plateau

The Central plateau zone has a moderate altitude and its topography is dominated by the hills and valleys with a warmer temperature of about 21°C (Bucagu, 2013). The sample area selected in Central Plateau is mainly covered by eucalyptus. The mean annual rainfall reaches up to 900 mm (Henninger, 2013).

Table 1: The area and average elevation of the sample areas

Date	**AEZ**	**Sample areas**	**Average elevation**	**Area**
21-06-2019	Eastern Savanna and Central Bugesera	Akagera savanna	1292m	71.7km2
14-07-2019	Central Plateau	Eucalyptus	1363m	0.3km2
15-08-2019	Congo-Nile Watershed Divide	Tea	1945m	0.85km2
15-08-2019	Congo-Nile Watershed Divide	Nyungwe forest	2368m	6.21km2

3.2. Data collection and description

3.2.1. Sample area selection

Sample areas of Akagera, Eucalyptus, Nyungwe and Tea were selected based on different landcover type, different location, elevation and the time (Month/Year) when cloud free Landsat 8 images and SMOS soil moisture data were acquired.

3.2.2. Satellite dataset

3.2.2.1. SMOS Level 2 soil moisture product

The Soil Moisture and Ocean Salinity (SMOS) is the first satellite to make passive observations specific to enable soil moisture retrieval and it was launched by the European Space Agency (ESA) on November 2, 2009 (Pierdicca et al., 2013). The payload of SMOS (European Space Agency, 2017) consists of the Microwave Imaging Radiometer using Aperture Synthesis (MIRAS) instrument, a passive microwave 2-D interferometric radiometer, operating in L-band (1.413 GHz, 21 cm) within a protected wavelength/frequency band. ESA's SMOS mission is based on a sun-synchronous orbit (dusk-dawn 6am/6pm) and it provides global measurements of L-band brightness temperatures, resulting in soil moisture with an accuracy of 0.04 m3m-3 at a spatial resolution of 35-50 km and a temporal sampling of 1-3 days (European Space Agency, 2017). SMOS provide soil moisture data at different levels and spatial resolution (European Space Agency, 2017), Level 2, Level 3 and Level 4. In this study, SMOS Level 2 (L2) soil moisture product was used with 3 days as temporal resolution. SMOS L2 data are geolocated products, delivered by the ESA on the Icosahedral Snyder Equal Area (ISEA) projection and they were sampled over the ISEA4h9 grid, which has a spacing in the order of 15 km (Sánchez et al., 2012). To ensure the best quality of SMOS soil moisture retrievals, SMOS L2 processing filters out the data strongly affected by Radio Frequency Interferences (RFI) (Pierdicca et al., 2013) and removes all unreliable values, such as negative soil moisture and soil moisture data with a Data Quality Index greater than 0.07 (Souza et al., 2018). SMOS Level 2 products are freely available in NetCDF format and they can be downloaded from https://smos-diss.eo.esa.int/oads/access/collection/SMOS_Open.

3.2.2.2. Landsat 8 Collection 2 Level 2 data

Landsat 8 is the most recently launched Landsat satellite (Acharya et al., 2017). It carries two instruments: The Operational Land Imager (OLI) and Thermal Infrared Sensor (TIRS) (USGS, 2013) and it provides atmospherically corrected products produced from Collection 2 Level-1 inputs. It generates several improvements in data processing and algorithm development including:

- Improved per-pixel geometric accuracy by incorporating updated Landsat 8 ground control points (GCP) harmonized with the Europe's Copernicus Sentinel-2 Ground Reference Image (GRI) which improves the interoperability of the global Landsat 8 archive spatially and temporally with other remotely sensed datasets.
- Improved calibration and validation updates
- Pixel based quality assessment bands.
- Updated global digital elevation modelling sources for various global regions

In this study, Landsat 8 collection 2 level 2 dataset was used. The dataset contains atmospherically corrected surface reflectance and land surface temperature. The output images have 5 visible and near-infrared (VNIR) bands, 2 short-wave infrared (SWIR) bands processed to orthorectified surface reflectance, one thermal infrared (TIR) band processed to orthorectified brightness temperature, intermediate bands used in calculation of the LST products and Quality Assessment (QA) masks indicating the usefulness of the pixel data (Sayler & Zanter, 2020).

Thermal infrared (TIR) band for collection 2 level 2 is acquired at 100 meter resolution, but is resampled to 30 meter in delivered data product (Acharya & Yang, 2017). The images can be retrieved from Earth Explorer at a spatial resolution of 30m with 16 days as temporal resolution. Cloud free images of both Nyungwe forest and tea were acquired on August 15th, 2019, Eucalyptus on July 14th, 2019 and the one for

Akagera savanna was acquired on June 21st, 2019. Landsat 8 Collection 2 Level 2 data can be downloaded freely from https://earthexplorer.usgs.gov/ in GeoTiff format.

3.2.2.3. WaPOR actual Evapotranspiration and Interception (ETIa)

FAO-WaPOR portal provide level 2 ETIa at 100m resolution. The data is in a GeoTiff format where the value of each pixel represents the average daily ETIa (in mm) provided per dekade. ETIa data was retrieved by choosing a dekade coinciding with the same date of the other input data for the investigated period. During the study period (June-August), the interception was zero for all the study areas, due to no rainfall occurrence, it was assessed using daily precipitation from FAO-WaPOR database for a continental level. FAO-WaPOR level 2 actual evapotranspiration and interception can be freely obtained online through FAO-WaPOR portal https://wapor.apps.fao.org/home/WAPOR_2/2.

3.2.3. Model dataset

Weather data used in this study were collected from the model generated datasets of ECMWF ERA5-Land hourly which is a reanalysis dataset covering the period from 1981 to present. Era5-Land provides a consistent view of the evolution of land variables over several decades at an improved resolution compared to ERA5. ERA5-Land data are freely available at 0.1° x 0.1° spatial resolution in both GRIB and NetCDF formats. They can be retrieved from https://cds.climate.copernicus.eu/cdsapp#!/dataset/reanalysis-era5-land?tab=form using appropriate scripts provided in the Climate Data Store Toolbox (CDSToolbox).

4. RESEARCH METHODOLOGY

4.1. Flowchart

Figure 3 below shows a general overview of the methodology approach. The description of the main activities including data preparation(SMOS L2 data, Landsat 8C2L2 data and ERA5-Land data), general approach of the triangle method for soil moisture estimation and different evapotranspiration methods (FAO-WaPOR, Penman-Monteith method and DATTUTDUT model) and their comparative analysis are described in the sections below.

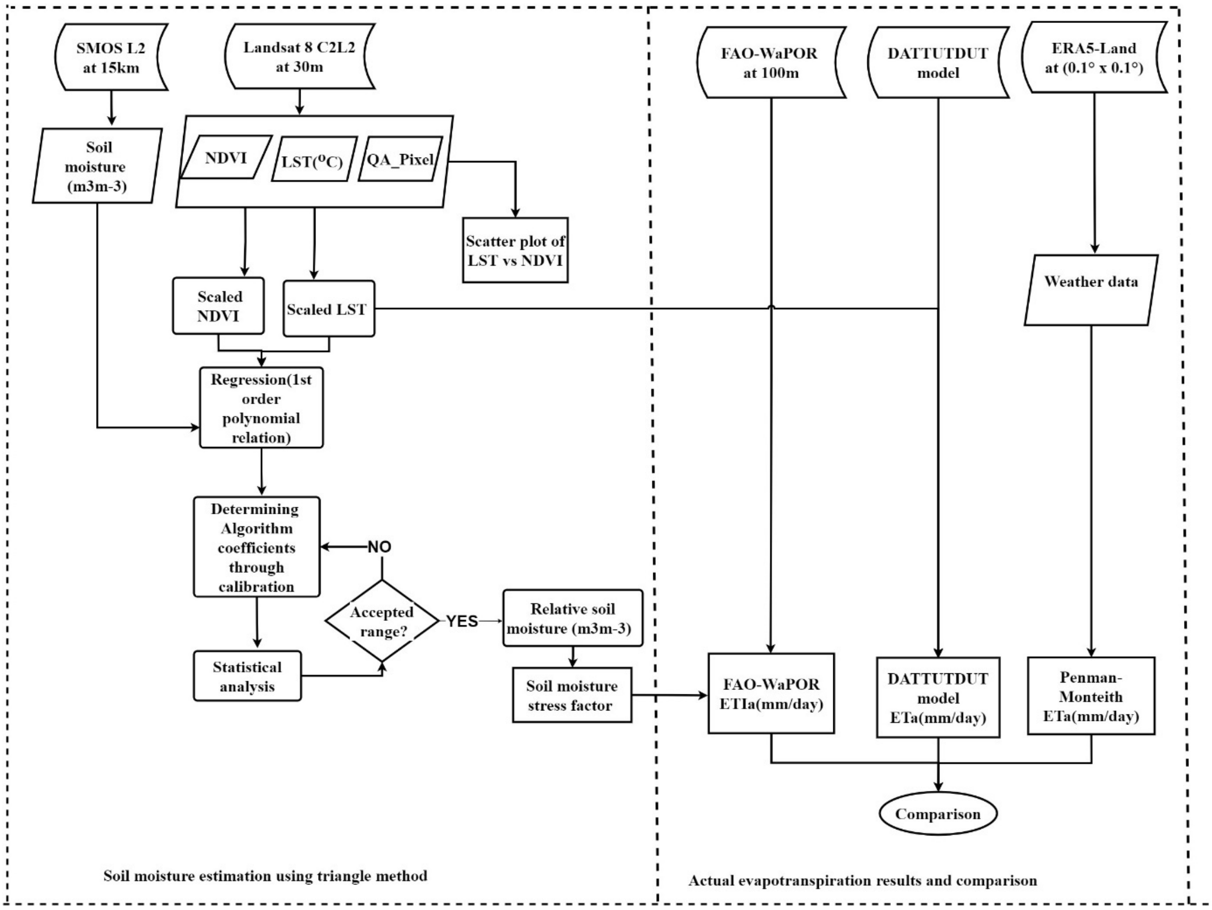

Figure 3: Flowchart

4.2. Data preparation

In this study, two types of data were used. Satellite data and model data. The data preparation was done to adjust the downloaded data to the same file format, same projection and same study area extent.

4.2.1. Satellite datasets

4.2.1.1. Landsat 8 collection 2 level 2 data

Pixel quality band (QA-Pixel) from Landsat 8 collection 2 level 2 data was used to filter NDVI and LST by removing clouds and open water. The process was done in ArcGIS using the Landsat_QA_ArcGIS_tool which helps to extract quality bands from the computed NDVI and LST. The Quality Assessment (QA) masks indicates the usefulness of the pixel data, it ranges from 0 (quality pixels) to 1(pixels with cloud cover and open water). Figure 4 below shows Cloud and water masking flowchart and sample area selection.

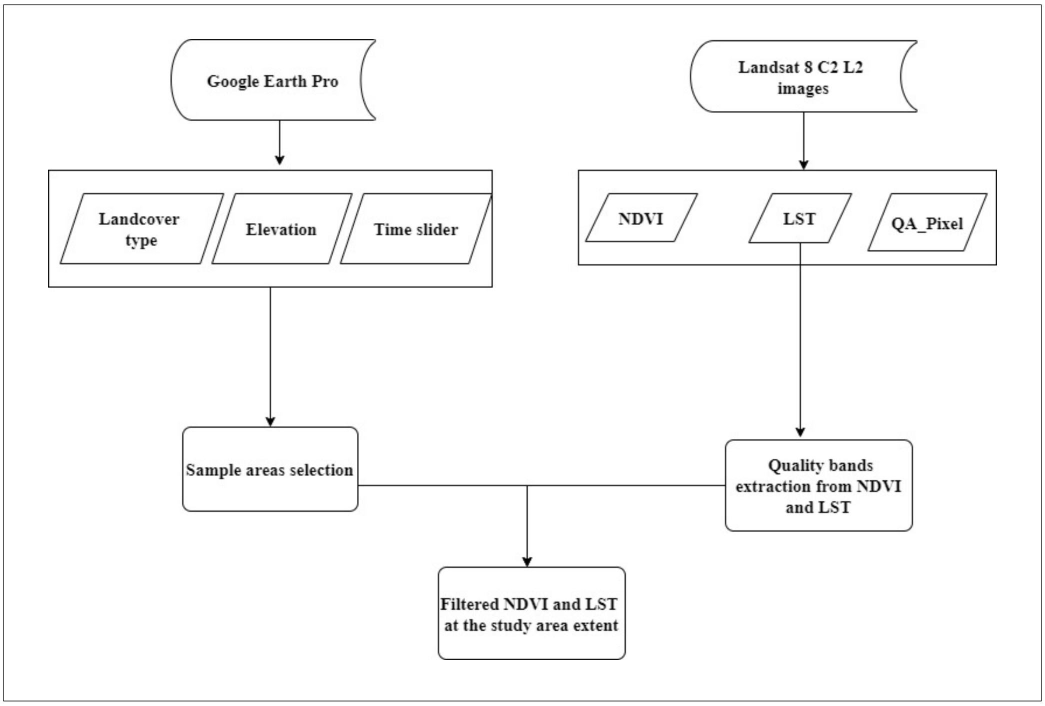

Figure 4: Cloud and water masking flowchart and sample area selection

4.2.1.2. SMOS Level 2 soil moisture product

Observed soil moisture used in this study was retrieved from SMOS L2 data as described in section (3.2.2.1). SMOS Level 2 data were opened in SNAP using the SMOS-toolbox, which is a SNAP extension dedicated to the exploitation of SMOS data. The output format of the soil moisture image was (IMG). GDAL was used to translate the IMG format into MPR format for the images to be processed in Ilwis where submaps of the study areas were created. The images were then exported as GeoTiff format for further processing in ArcGIS.

4.2.2. Model datasets

4.2.2.1. Weather data

Weather data used in this study were directly retrieved from ERA5-Land using ERA5-Land toolbox with the help of appropriate python scripts provided in appendix 2. The downloaded data (10m u and v-component of wind speed at 10m, maximum (max) and minimum (min) air temperature and dew temperature) were then visualized using Panoply to collect the necessary information needed to the import the data in ILWIS using GEONETCast toolbox-C3SCDS-ERA5 Import. The imported data needed for the calculation of Penman Monteith equation were hourly data, they were then converted to daily. Max and min air temperature and dew temperature were converted into ^{0}C.

For the calculation of evapotranspiration, wind speed measured at 2 m above the surface is required. The downloaded wind speed at 10m was adjusted to wind speed at 2m using the formulas below suggested by Allen et al. (1998).

$$U10 = \sqrt{u_{10}^2 + v_{10}^2} \qquad \text{Equation 10}$$

Where U10 is wind speed at 10m above ground surface, u_{10} is Eastward component of the 10m wind, v_{10} is Northward component of the 10m wind.

$$u2 = u_z \frac{4.87}{\ln(67.8z - 5.42)} \qquad \text{Equation 11}$$

where u2 is wind speed at 2 m above ground surface [m s-1], uz measured wind speed at z m above ground surface [m s-1] and z height of measurement above ground surface [m].

4.3. General approach of the triangle method for soil moisture estimation

According to Rahmati et al. (2015b), the triangle method is a step by step algorithm that is performed based on:

1. Observed soil moisture,
2. Computation of the NDVI and LST from satellite images,
3. Scaling the computed NDVI and LST to NDVI* and LST*,
4. Constructing polynomials between the observed soil moisture and NDVI* and LST*.
5. Mapping the estimated soil moisture.

Step 1: SMOS soil moisture

Table 2 shows the number of pixels covered by sample areas on the SMOS grid and the soil moisture values used in this study for all the sample areas. These values have been manually retrieved using an overlay with the sample areas.

Table 2: Number of pixels covered by sample areas on the SMOS grid

Sample area	Date	Pixels	SMOS soil moisture (m3m-3)
Akagera savanna	21-06-2019	3	0.21
Eucalyptus	14-07-2019	1	0.16
Tea	15-08-2019	1	0.30

Step 2: Computation of NDVI and LST from Landsat 8 C2 L2 data

NDVI

The computation of Normal Difference Vegetation Index (NDVI) was done using Band 5 and Band 4 Surface Reflectance (SR) of Landsat 8 C2 L2 OLI data. The below formula was used (Kristi Sayler, 2020):

$$NDVI = \frac{NIR(Band\ 5\ SR) - R(band\ 4\ SR)}{NIR(Band\ 5\ SR) + R(Band\ 4\ SR)} \qquad \text{Equation 12}$$

where NIR represents the near-infrared surface reflectance Band (Band 5 SR) and R represents the red surface reflectance band (Band 4 SR).

LST

The retrieval of LST (in K) from Landsat 8 C2 L2 was done by multiplying Band 10 provisional Surface Temperature (ST) with a multiplicative scale factor of 0.00341802 and by adding 149 as an additive scale factor (Kristi Sayler, 2020). The result was then converted into ^{o}C by subtracting 273.15.

$$LST = (Band10\ ST * 0.00341802 + 149) - 273.15 \qquad \text{Equation 13}$$

where LST is the atmospherically corrected land surface temperature and Band 10 ST is the provisional Surface Temperature (ST).

Step 3: Scaling NDVI and LST to NDVI* and LST*

The scaling of NDVI and LST reduces the sensitivity of NDVI and LST to atmospheric correction and calibration issues, helps to isolate cloud and water pixels which tend to lie outside the triangle. Computed NDVI and LST were scaled using respectively maximum and minimum NDVI and LST found inside the triangle from scatter plot. The maximum and minimum values for both NDVI and LST can be related simply by observing the scatter plots between the computed NDVI and LST .

$$LST^{*} = \frac{LST - LST_{min}}{LST_{max} - LST_{min}} \qquad \text{Equation 14}$$

$$NDVI^{*} = \frac{NDVI - NDVI_{min}}{NDVI_{max} - NDVI_{min}} \qquad \text{Equation 15}$$

Where NDVI* and LST* are scaled NDVI and scaled LST respectively, LSTmax and NDVImax are respectively maximum LST and NDVI and NDVImin and LSTmin are minimum NDVI and LST respectively found inside the triangle from scatter plot.

Step 4: Construction of polynomials between the observed soil moisture and NDVI* and LST*

The 1st order polynomial relation was used to estimate soil moisture from remote sensing by relating the observed soil moisture with scaled NDVI and LST. The equation has a total of 4 coefficients. NDVI and LST maps are produced first and their scatter plots were formed through crossing in ILWIS. From the scatter plots, the minimum and maximum values of NDVI and LST are determined which were further used to scale LST and NDVI by applying equation 14 and 15 respectively. After scaling NDVI and LST, the polynomial relation was formed between the observed soil moisture with scaled NDVI and LST at pixel level as follows:

$$SM = a_{00} + a_{01}NDVI^* + a_{10}LST^* + a_{11}NDVI^*LST^* \qquad \text{Equation 16}$$

Where SM is estimated soil moisture, NDVI* and LST* are respectively scaled NDVI and scaled LST, a00, a01, a10 and a11 are polynomial relation coefficients.

Step 5: Calibration

Calibration is performed to ensure that the triangle method produced accurate results for the estimation of soil moisture content and stress factor. Here, parameters were calibrated for better simulation of results when they are related to observed data. To define the nth order of polynomial relation, the coefficients were calibrated by comparing the estimated soil moisture with the SMOS soil moisture until the estimated shows an acceptable accuracy. SMOS soil moisture has a resampled spatial resolution of 15km, therefore only few pixels could be manually selected based on each sample area extent. As mentioned in Table 2, 3 pixels were selected for Akagera savanna, 1 for tea and 1 for eucalyptus.

The root mean square error (RMSE) was used to measure the level of agreement between the estimated soil moisture and SMOS soil moisture. RMSE is calculated using the following formula:

$$RMSE = \sqrt{\frac{\sum_{i=1}^{n}(SM - SM_{SMOS})^2}{n}} \qquad \text{Equation 17}$$

Where RMSE is the root mean square error, SM_{SMOS} is the SMOS soil moisture, SM is the estimated soil moisture and N is the number of samples.

Step 6: Estimation of soil moisture stress factor

Estimation of soil moisture stress factor was done using Equation 9. Table 3 shows the tenacity factor (Ksf) used for each sample area based on (FAO, 2018a).

Table 3: Tenacity factor (Ksf)

Date	**Sample area**	**Ksf**
21-06-2019	Akagera savanna	1.5
14-07-2019	Eucalyptus	3
15-08-2019	Tea	3

4.4. Penman-Monteith actual evapotranspiration

The Equation 1 was used to calculate the reference evapotranspiration using FAO-56 Method (Allen et al., 1998). The computation was done following step by step calculation of Penman-Monteith evapotranspiration described by Zotarelli et al. (2014) using weather data obtained from ERA5-Land. The process was done in excel. To get the ETa for all the sample areas, Equation 2 was used. Table 4 shows the Kc values provided by Allen et al. (1998). The Kc values of tea and eucalyptus are higher than that of Akagera savanna because tea and eucalyptus don't have seasonal influence. They remain the same in both cool and dry season. The used Kc for tea is 1.33 and 1 for eucalyptus. Unlike tea and eucalyptus, Akagera savanna is much affected by seasonal influence, since the area is dominated by grassland savanna, they change in both dry and wet season. The Kc used for Akagera is 0.88.

Table 4: Crop coefficient (Kc)

Date	Sample area	Kc
21-06-2019	Akagera savanna	0.88
14-07-2019	Eucalyptus	1
15-08-2019	Tea	1.33

4.5. FAO-WaPOR actual evapotranspiration and interception (ETIa)

The FAO-Frame toolbox in ILWIS was used to import and process ETIa from FAO-WaPOR. In this research, Level 2 ETIa at 100m resolution was retrieved for all the sample areas.
The downloaded ETIa from FAO-WaPOR were provided per dekade, they were converted to the proper unit (mm) using the conversion factor of 0.1 to get daily average ETIa. The interception was zero for the study period (June-August).

4.6. Actual evapotranspiration (ETa) from Dattutdut model

The DATTUTDUT algorithm is simple to use and it provides a rapid estimate of spatially distributed fluxes provided a cloud-free and atmospherically corrected surface temperature image is available (Timmermans et al., 2015). Cloud free LST were first produced using Equation 13. The process is done in Ilwis using provided model script (Appendix 1). The code could be edited by changing four parameters (LST+0.5% offset minimum and maximum values of the LST image, UTC and its DoY of image acquisition.

4.7. Validation of FAO-WaPOR ETIa

The validation of FAO-WaPOR ETIa was done by investigating the crucial application of the triangle method in FAO-WaPOR ETIa methodology and by comparing the average ETIa from FAO-WaPOR ETIa to the average ETa derived from Penman-Monteith method and DATTUTDUT model.

4.8. An overview of the software used

In this research, several software packages were used for various tasks, at different stages of the research. The main ones are outlined below:

- **Panoply:** Panoply is a cross-platform application that was used for data visualization
- **GDAL:** The geospatial data abstraction library was used to translate raster datasets into same, common raster formats for visualization and analysis in different GIS environments and ILWIS.
- **ILWIS386:** The integrated Land and Water Information System was used for the acquisition of WaPOR ETa level 2 data using FAO-Frame toolbox, importing weather data from Era5-Land using GEONETCast toolbox-C3SCDS and for image manipulations.
- **ArcMap:** Different ArcMap tools were used to display, analyse raster data and to create map layouts for all study areas.
- **Python:** Climate Data Store Toolbox (CDS-Toolbox), a python coding environment was used to retrieve weather data from ERA5-Land.
- **SNAP:** The SMOS Toolbox (SMOS-Box) for Sentinel Application Platform (SNAP) developed for data acquired by ESA's SMOS mission was used to display and visualise SMOS Level-2 products.

- **Google Earth pro:** Google Earth pro was used to select sample areas by choosing homogeneous landcover type located at approximately the same elevation and by considering the time (Month/Year) when the Landsat 8 images and SMOS soil moisture data were acquired.
- **Microsoft office:** Excel was used though the process of creating scatter plots, estimating the regression coefficients used to estimate the soil moisture and estimating ETo and ETa using Penman-Monteith equation. Word was used for writing thesis report and Power Point was used for presentation.

5. RESULTS AND DISCUSSION

5.1. NDVI and LST results

5.1.1. NDVI

NDVI was computed from Landsat 8 C2 L2 OLI images of 15th August 2019 for both Nyungwe forest and tea, 21st June 2019 for Akagera savanna and 14th of July for eucalyptus using Equation 12. The result values are within 0 to 1 range and they are relatively low because only the dry season could be considered given cloud cover constraints during the other seasons. Table 5 shows the minimum and maximum and average NDVI of all the study areas. The process was done in ArcGIS. Tea showed highest average value of NDVI (0.41). Nyungwe forest showed the lowest NDVI value probably because the topography caused some part of the forest to be in the shade or the forest structure produced dark gaps in which even Near Infra-Red radiation is low.

Table 5: NDVI values for Akagera, Nyungwe and tea sample areas

Day	Sample area	$NDVI_{min}$	$NDVI_{max}$	Average
21-06-2019	Akagera	0.24	0.43	0.32
14-07-2019	Eucalyptus	0.23	0.34	0.31
15-08-2019	Nyungwe	0.19	0.43	0.29
15-08-2019	Tea	0.33	0.46	0.41

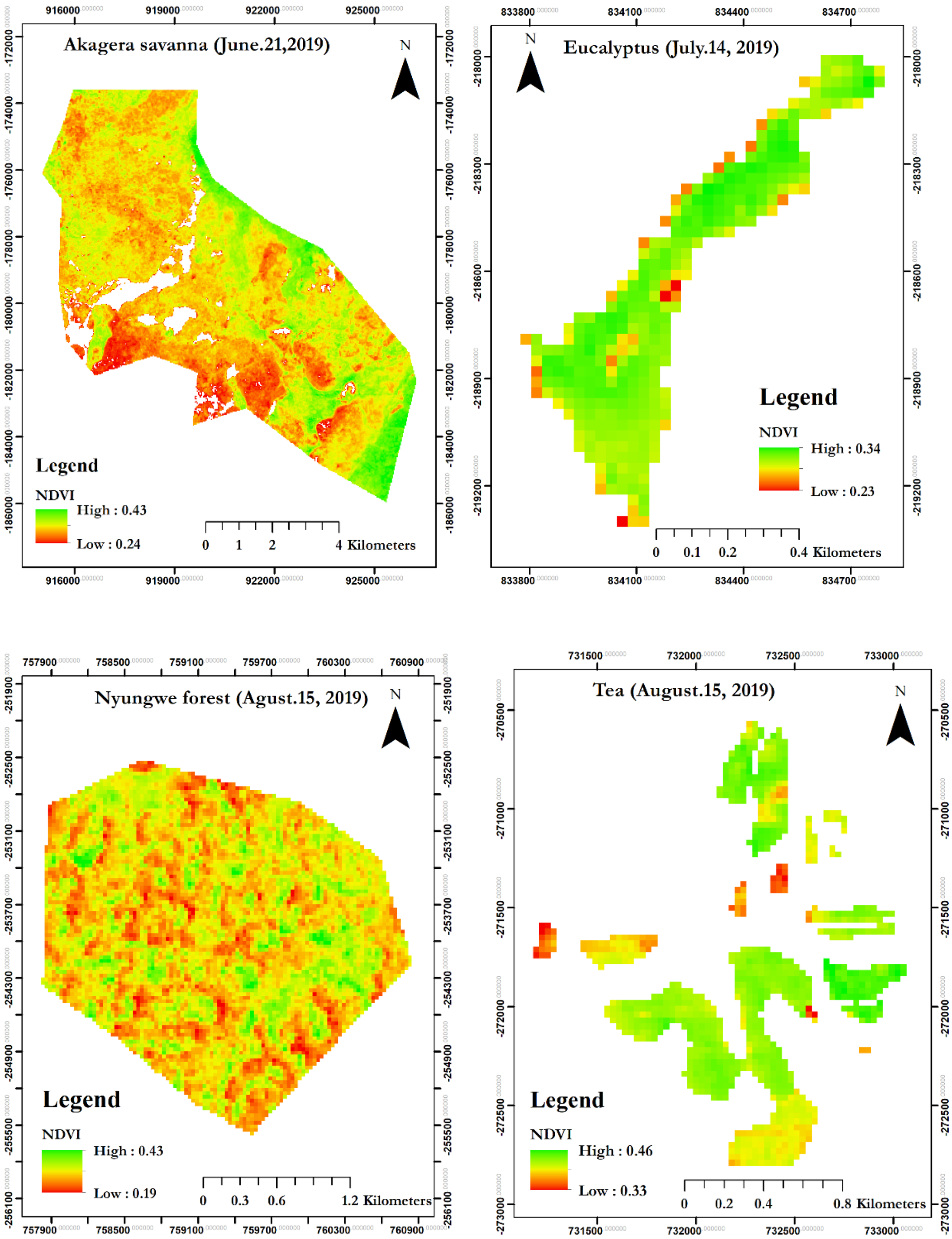

Figure 5: NDVI maps of sample areas

5.1.2. LST

Land surface temperature was derived using Equation 13. Eucalyptus showed highest average value of LST (27.11 °C) among all the sample areas probably because July is the driest of the year month in Rwanda. Table 6 shows the minimum, maximum and average LST of all the study areas.

Table 6: LST values for Akagera, Nyungwe and tea sample areas

Day	**Sample area**	**LST$_{min}$(°C)**	**LST$_{max}$(°C)**	**Average**
21-06-2019	Akagera savanna	19.2	25.1	20.6
14-07-2019	Eucalyptus	25.5	30.8	27.1
15-08-2019	Nyungwe	12.5	16.8	14.6
15-08-2019	Tea	12.7	16.5	13.9

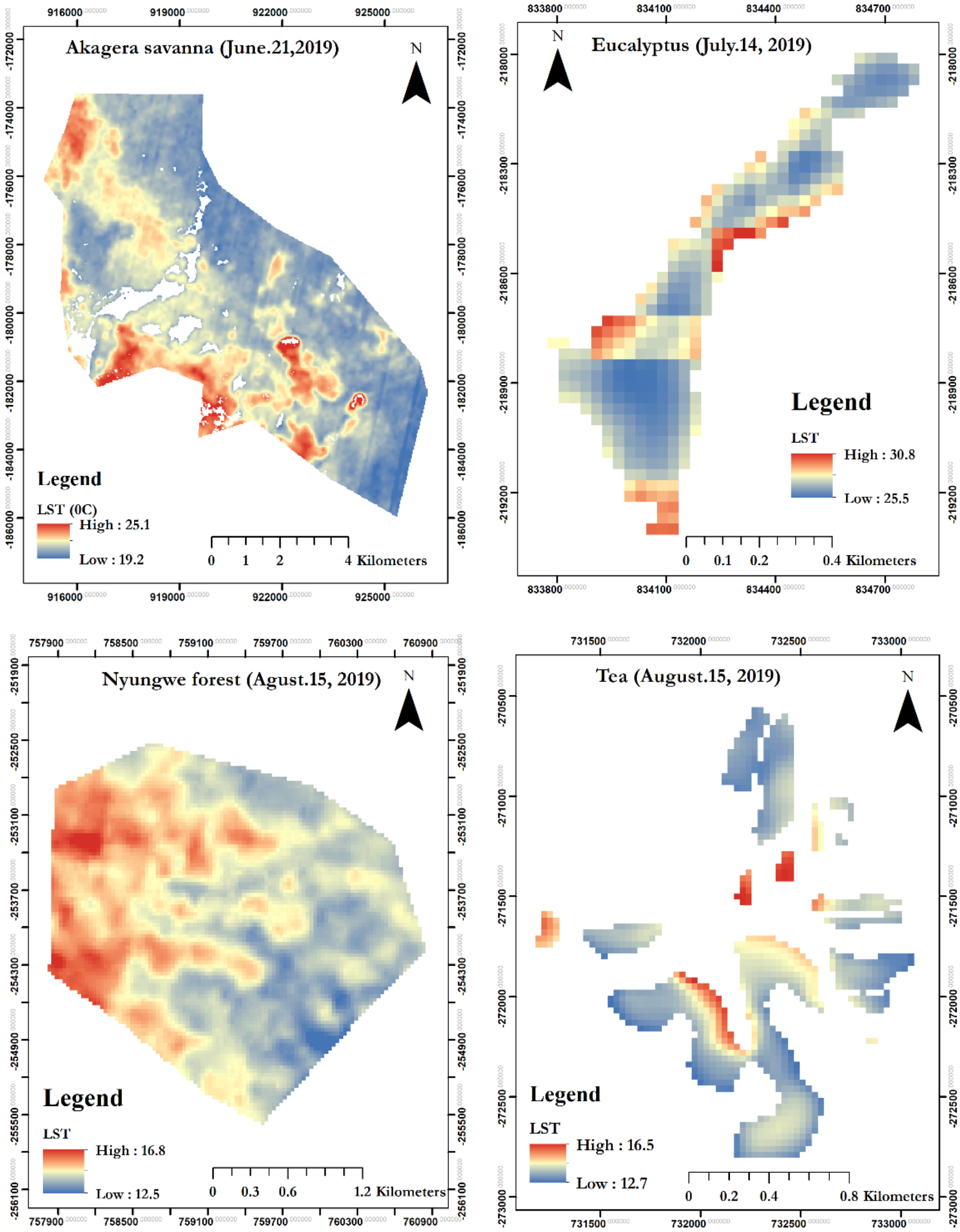

Figure 6: LST maps of sample areas

5.2. Scatter plots of NDVI and LST

Scatter plot of NDVI vs LST were made in ILWIS by crossing images of NDVI and LST Figure 5 and Figure 6 respectively, to determine the cold and warm edges and to show how the shape of the triangle varies for all the study areas. As identified in Figure 7, the scatter plots of Akagera (A), tea (B) and eucalyptus (C), the highest and lowest values of LST are indicated respectively as LSTmax and LSTmin and for NDVI, as NDVImax and NDVImin. The scatter plots of NDVI versus LST of Akagera, Tea and Eucalyptus show that the range of NDVI and LST variability is sufficient to define the triangle shape because within the triangle shape, NDVI and LST have negative relations for most pixels. LST decreases with the increasing NDVI values, especially near the warm edge. The cold and warm edges shown in the scatter plots correspond to the wettest and driest pixels respectively. The warm edge, defined by visual inspection of the pixel distribution from the scatter plot, represents the limit of soil surface dryness for a given vegetation amount. It represents the low evapotranspiration line or dry condition. The cold edge represents maximum soil wetness (Mekuria, 2012).

The location of a pixel in the scatter plot is influenced by many factors. Evapotranspiration and soil moisture availability are some of the factors. The pixels with less evaporation have high LST because the lower evaporation rate, the less latent heat is removed from the surfaces. On the other hand, soil moisture availability indirectly influences the location of the pixels in the scatter plot by controlling transpiration. The drier the soil surface, the less the transpiration.

The triangle method was best applied for Akagera savanna because from the scatter plot three important properties of the triangle method were observed. The first observation is the soil moisture variation from the right to the left side of the triangle where the right (warm edge) side of the triangle has low soil moisture and the left (cold edge) side of the triangle has high soil moisture. The second observation is the slope toward the left where the LST decreases as the NDVI increases especially on the warm edge of the triangle. The third and most important observation is on the apex of the triangle where the value of NDVI is higher but the corresponding value of LST is low with small variation, it is mentioned as point A on the scatter plot.

As shown in the scatter plot of Nyungwe Figure 7 (D), the triangle method is not applicable because there is no edge to be found (no warm or cold edge in the scatter plot). There is no limiting factor related to soil moisture probably because Nyungwe is considered as moist evergreen forest. Therefore, there is always sufficient soil moisture. Nyungwe forest was not considered for further analysis.

The triangular shape was well formed in Akagera savanna because the area is large enough to provide wide range of NDVI values from bare soil to vegetated surfaces and the soil moisture from wet to dry condition. Table 7 shows statistics on number of pixels used to produce scatter plot of each sample area

Table 7: Statistics on number of pixels and average elevation of each sample area.

Sample areas	Number of pixels	Average elevation
Akagera savanna	75736	1292m
Eucalyptus	183	1363
Tea	929	1945
Nyungwe forest	6893	2368

It is easy to understand the relationship of NDVI-LST using a scatter plot but because the boundary of polygon is highly dependent on many factors like surface physical variables and atmospheric properties, it was difficult to clearly draw unique lines for cold and warm edges

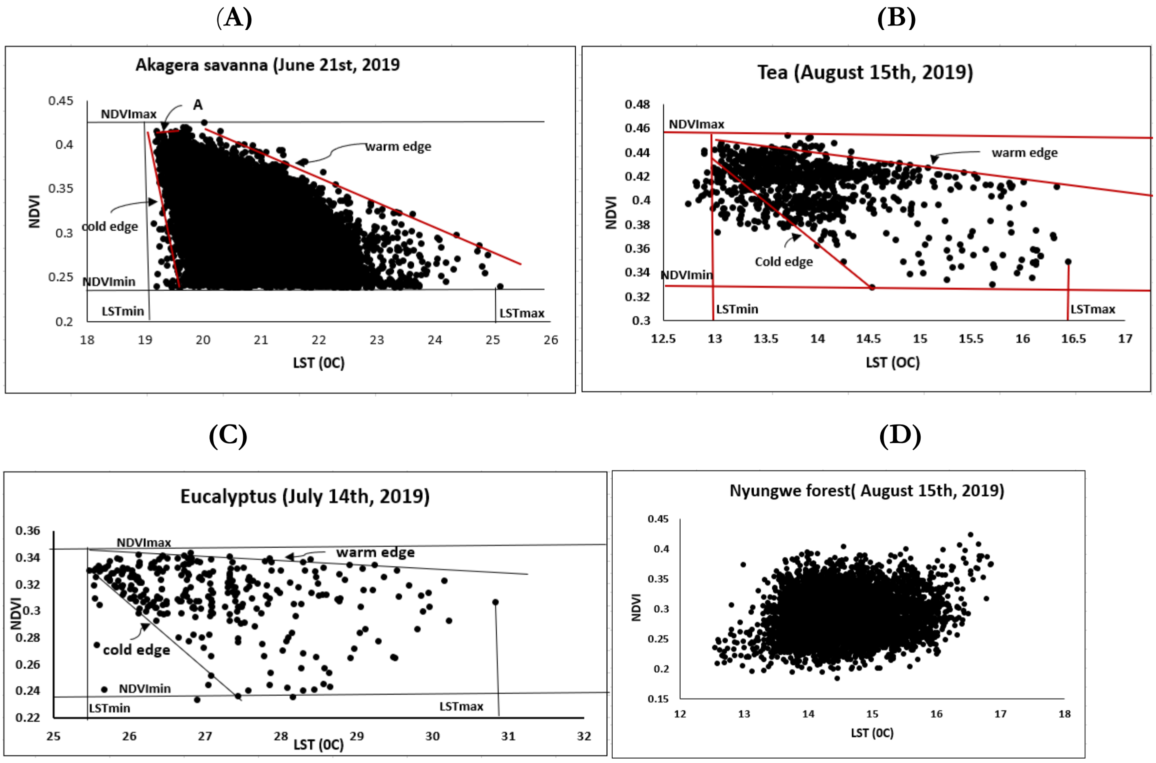

Figure 7: Scatter plot of Akagera savanna(A), tea (B), eucalyptus (C) and Nyungwe forest (D)

5.3. Relative soil moisture content and soil moisture stress factor results

Relative soil moisture content is estimated from the relationship between LST, NDVI and the observed soil moisture using the suggested triangle method. The relationship was derived applying Equation 16. Three pixels were identified for Akagera and one tea and eucalyptus. All the sample areas indicated the best result after calibration where the estimated soil moisture showed the same tendency as SMOS soil moisture. The coefficients aij from Equation 1 for the algorithm obtained after calibrations for all sample areas are presented in Table 7. The results of the comparison between the estimated and SMOS soil moisture are presented in Table 8 for Akagera savanna, tea and eucalyptus. The values of SMOS soil moisture and estimated soil moisture are relatively close and their RMSEs are close to SMOS mission target accuracy 0.04 m3m-3. The average estimated soil moisture are relatively low because it was a dry season and no rain was present at the moment for all the periods the data were collected. Table 9 shows the soil moisture stress factor (Sm) for all the sample areas and the results indicated that all sample areas are under soil moisture stress conditions because their soil moisture stress factor is less than 1. Figure 8 shows estimated soil moisture maps (30m spatial resolution) of all sample areas.

Table 8: Coefficients for 1st order polynomial relation

Study area	a_{00}	a_{01}	a_{10}	a_{11}
Akagera	2.57	0.05	0.60	0.90
Eucalyptus	5.98	0.0002	0.10	0.90
Tea	16.77	0.02	0.60	0.76

Table 9: Analysis of the estimated soil moisture and SMOS soil moisture

Date	Sample area	SMOS soil moisture (m3m-3)	Estimated soil moisture (m3m-3)	RMSE (m3m-3)	Pixels
21-06-2019	Akagera savanna	0.208	0.206	0.043	3
14-07-2019	Eucalyptus	0.163	0.162	0.031	1
15-08-2019	Tea	0.3	0.29	0.043	1

Figure 8 demonstrates the spatial variability in soil moisture (m^3m^{-3}) of all the sampled areas during the investigated dry season (June-August). It can be seen that the eucalyptus trees show less differences in spatial patterns of soil moisture (more or less homogenous). The tea area is showing spatial variation in soil moisture, a high soil moisture in the middle of the tea field (around $0.32m^3m^{-3}$) and a low soil moisture ($0.28m^3m^{-3}$) in the surrounding. This is probably due to the fact that the surrounding areas are located near Nyungwe forest where thick trees with long roots are found. These trees with long roots absorb more water from the soil thus affecting the surrounding tea area. Akagera savanna is demonstrating high spatial distribution in soil moisture, which can be explained by the heterogeneity of the area (a mixture of grass, trees, water bodies and bare soils) . Areas with trees and areas located near water bodies showed high soil moisture content while areas with bare soils and grasses showed low soil moisture content.

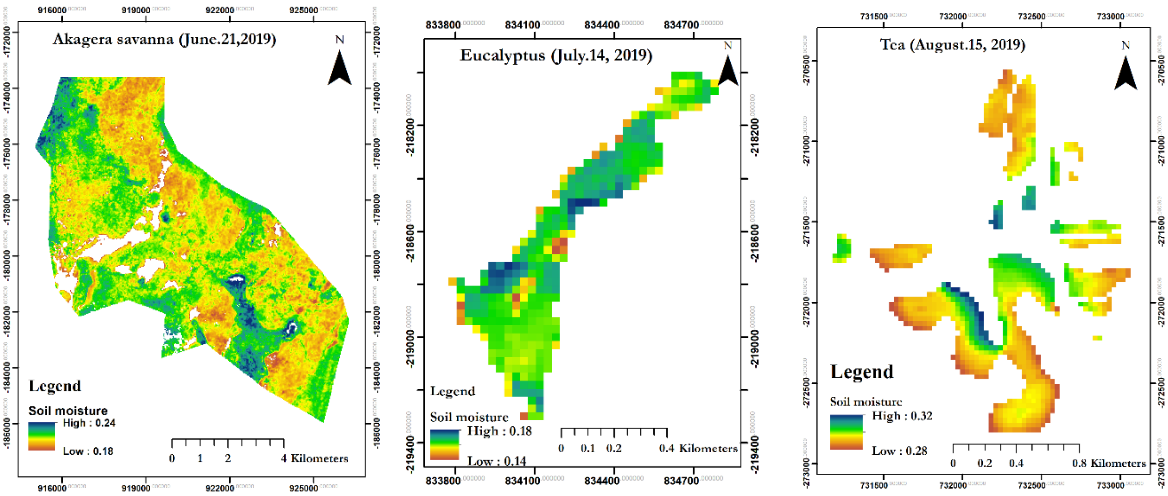

Figure 8: Estimated soil moisture maps for Akagera savanna (left), eucalyptus(middle) and tea(right).

Table 10: Soil moisture stress factor result

Date	Sample area	Soil moisture stress factor (S_m)
21-06-2019	Akagera savanna	0.15
14-07-2019	Eucalyptus	0.35
15-08-2019	Tea	0.73

5.4. Actual evapotranspiration (ETa) result

ETa was derived from Penman-Monteith (PM) method and DATTUTDUT model and retrieved from FAO-WPOR database. The results in Table 10 showed that the three methods have realistic values with slightly deviating values less than 1mm/day. Among the three methods, the ETa values of the DATTUTDUT model have limited variability, the ETa values are quite similar despite the fact that the land cover types and climate are different because DATTUTDUT model does not use neither NDVI nor weather data like other methods to derive ETa, it only use a LST. As shown in Figure 9, there is a relationship between DATTUTDUT model ETa maps and LST maps. The spatial distribution of ETa within the sample areas is the same as the one of LST. Areas with low LST reflected high ETa while areas with high LST reflected low ETa. On the other hand, the spatial distribution of FAO-WaPOR ETIa within the sample areas is the same as NDVI spatial distribution as shown in Figure 10. The areas with high NDVI reflected high ETIa while areas with low NDVI reflected low ETIa.

Table 11: Actual evapotranspiration results

Sample areas	Date	ETa_PM (mm/day)	ETIa_FAO-WaPOR (mm/day)	ETa_DATTUTDUT (mm/day)
Akagera	21-06-2019	3.38	3.97	4.71
Eucalyptus	14-07-2019	3.57	3.56	4.32
Tea	15-08-2019	5.98	5.08	4.52

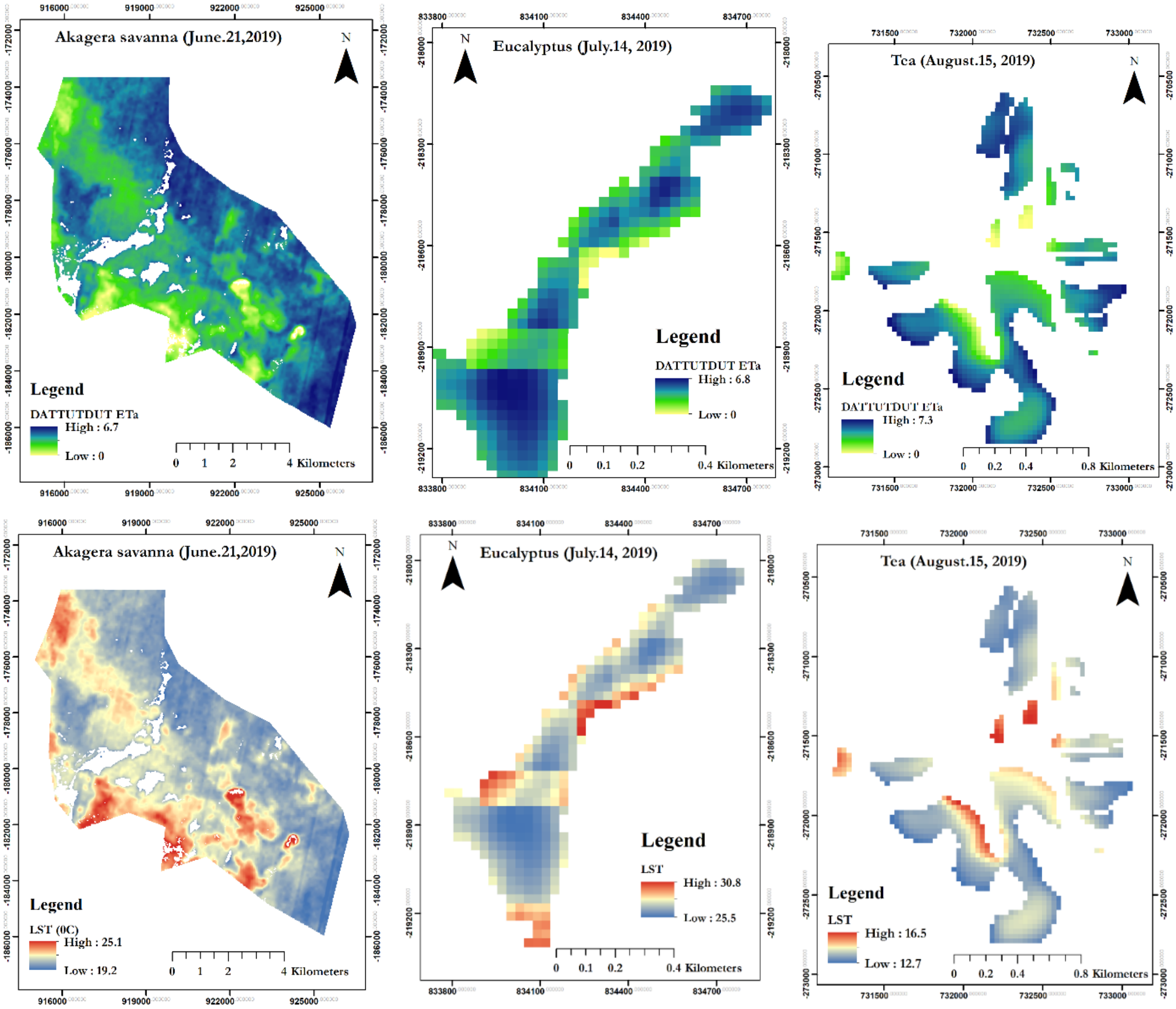

Figure 9: Relationship in spatial distribution of DATTUTDUT model ETa and LST maps

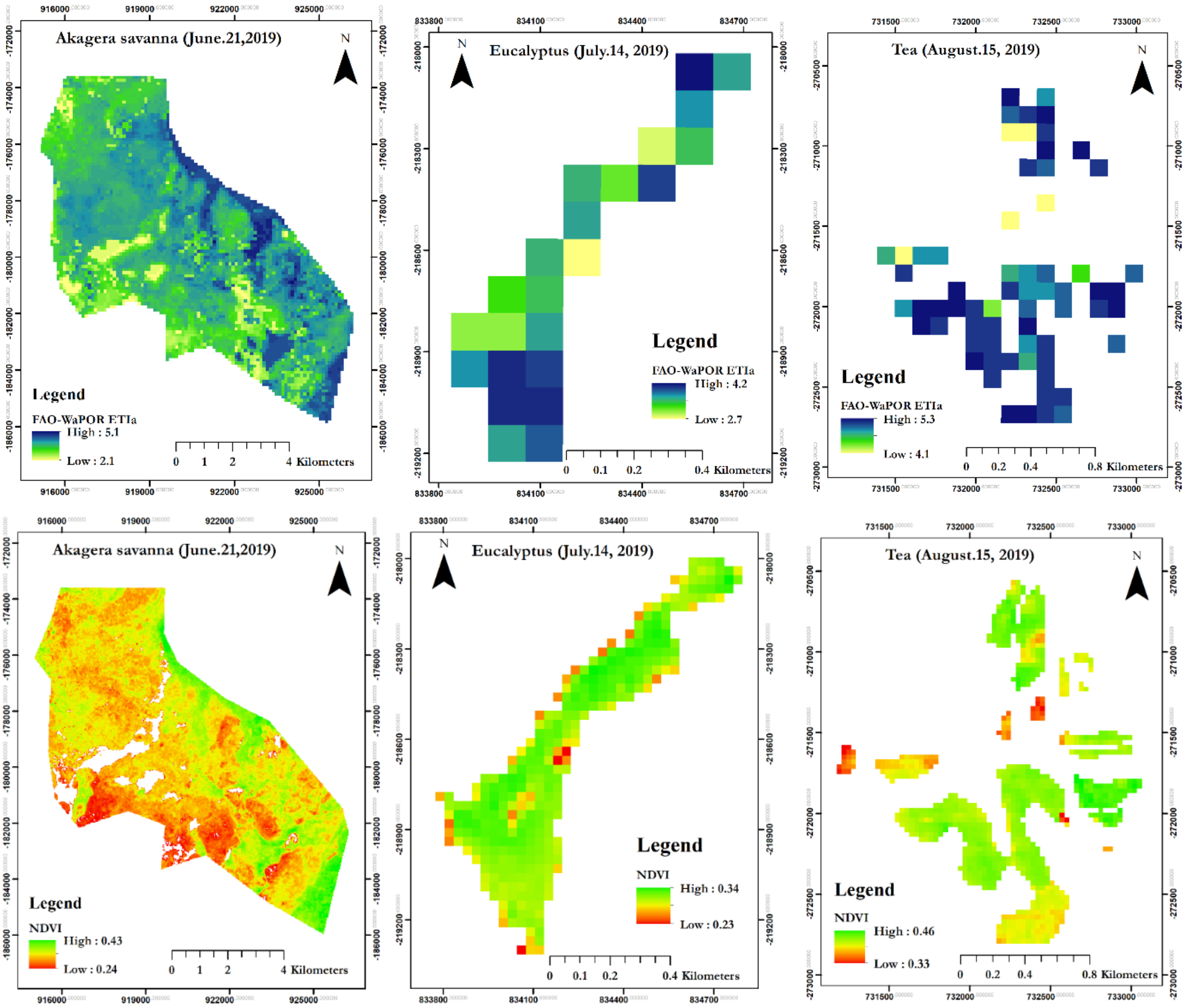

Figure 10: Relationship in spatial distribution of FAO-WaPOR ETIa and NDVI maps

5.4.1. Comparative analysis of Penman-Monteith ETa and FAO-WaPOR ETIa

As shown in Table 10, the results of Penman-Monteith ETa and FAO-WaPOR ETIa are realistic and relatively close to each other with slightly deviating values less than 1mm/day. Both Penman-Monteith method and FAO-WaPOR indicated high value of actual evapotranspiration for tea (5.98mm/day and 5.08mm/day respectively) compared to the other two sample areas. This is due to the fact that tea is located in the lowest average temperatures with high average relative soil moisture content and high average NDVI value compared to the other two sample areas. The area with high NDVI values and low LST values tends to have maximum transpiration and maximum evaporation respectively. The ETa for tea takes place at maximum rate and LST is close to the ambient air temperature.

5.4.2. Comparative analysis of DATTUTDUT model ETa and FAO-WaPOR ETIa

DATTUTDUT model doesn't use neither NDVI nor weather data to estimate ETa, it is solely based on a LST image acquired over the area of interest. As shown in table 10, when using DATTUTDUT model, ETa value of Akagera savanna and eucalyptus increased by less than 1mm/day and the one of tea reduced by less than 1mm/day. The reason of this increase and decrease in ETa values is because of the difference in evaporative fraction (LSTmax-LST/LSTmax-LSTmin) within the image among locations.

5.4.3. Evaluation of the soil moisture stress effect on FAO-WaPOR ETIa

FAO-WAPOR uses the triangle method information (soil moisture stress) to reduce ETIa. Without including the soil moisture stress factor, FAO-WaPOR appears to overestimate ETIa. The evaluation was done by dividing the ETIa with the soil moisture stress factor. ETIa of Akagera savanna has increased by 22.53mm/day, eucalyptus by 6.64mm/day and tea by 1.82mm/day. The results shows that the sensitivity of ETIa to stress is very high when having soil moisture stress factor with lower values. Table 11 shows the effect of soil moisture stress on FAO-WaPOR ETIa.

Table 12: Effect of soil moisture stress on FAO-WaPOR ETIa

Date	**Sample areas**	**Soil moisture tress factor**	**FAO-WaPOR ETIa (mm/day)**
21-06-2019	Akagera savanna	0.15	26.5
14-07-2019	Eucalyptus	0.35	10.2
15-08-2019	Tea	0.73	6.9

6. CONCLUSION AND RECOMMENDATION

6.1. Conclusion

The main objective of this study was to evaluate the application of the triangle method for different agro-ecological zones of Rwanda and to determine how it affects actual evapotranspiration (ETa), key parameter used to determine the Water Productivity provided by FAO-WaPOR. In this research, triangle method was investigated on four landcover types (Akagera savanna, Nyungwe forest, tea and eucalyptus) to derive their relative soil moisture content and soil moisture stress factor which provided additional information that are relevant for a better estimation of FAO-WaPOR actual evapotranspiration under soil moisture stress conditions.

The triangle method was first established by showing the relationship between the LST and NDVI for all the sample areas, to get an idea of the soil moisture availability according to the cold and warm edges formed inside the scatter plot except for Nyungwe forest. The estimation of the relative soil moisture was done by relating the soil moisture from SMOS level 2 , Normalized Difference Vegetation Index (NDVI) and Land Surface Temperature (LST) retrieved from remote sensing. The triangle method provided a good estimation of the soil moisture at high spatial resolution (30m) for all sample areas with averaged RMSEs relatively close to the SMOS mission target accuracy of 0.04m3m-3. From the estimated relative soil moisture content, soil moisture stress factor (Sm) was derived. The result of the triangle method (soil moisture stress factor) indicated that all the sample areas are under soil moisture stress conditions, Akagera savanna area has the lowest Sm value of 0.15, eucalyptus has a Sm of 0.35 and tea has the highest Sm value of 0.73.

Soil moisture stress factor (Sm) is one of the factors affecting actual evapotranspiration. FAO-WaPOR ETIa values were much affected by soil moisture stress conditions especially in areas with low Sm values. Thus resulting in FAO-WaPOR ETIa overestimation. ETIa of Akagera savanna has increased by 22.53mm/day, eucalyptus by 6.64mm/day and tea by 1.82mm/day. The above results indicated that with lower Sm values, the effect is very large. Therefore, a small adjustment in Sm values has a major impact on FAO-WaPOR ETIa. Blatchford et al. (2020) conducted a study on the evaluation of WaPOR V2 evapotranspiration products across Africa, their findings showed that ETIa-FAO-WaPOR was performing well, but with some noticeable overestimation. They concluded that FAO-WaPOR seemed to overestimate ETIa under soil moisture stress conditions.

The validation of the FAO-WaPOR ETIa was done by comparing the FAO-WaPOR ETIa to the ETa derived from Penman-Monteith method and DATTUTDUT model. The comparative analysis indicated that despite their difference in spatial resolution, the results of the three methods are comparable and relatively close to each other.

6.2. Limitations of the study

The main limitations of this study are listed below:

- Few Landsat 8 C2 L2 cloud free data due to the dependency on the thermal infra-red data for the investigated period (June-August)). This limited the number of SMOS soil moisture sample points.
- Soil moisture stress factor, NDVI and LST data are not yet made available by FAO-WaPOR database.
- There have been limited studies in various areas in Africa (for example: Ethiopia) which cannot be compared to Rwanda due to the difference in climate.
- No in-situ data were available for validation.
- Data with different spatial resolution.

6.3. Recommendation

- FAO-WaPOR open portal does not publish the data source of the parameters used to produce their ETIa product, it is recommended for FAO-WaPOR to provide the lacking information for future researchers to accurately assess these parameters.
- There have been limited studies on the investigation of the triangle method in various areas in Africa. Therefore, further studies are recommended.
- This study was carried out during a dry season of the year (June-August) with a shortage of available cloud free images, further study is recommended to improve the investigation of the triangle method by taking enough ground measured soil moisture in both dry and wet seasons.

LIST OF REFERENCES

Acharya, T. D., & Yang, I. (2017). *Exploring Landsat 8. May 2015.*
African Water Facility. (2016). *Rwanda National Integrated Water Supply and Sanitation Master Plans Project Appraisal Report November 2016. November*, 1–67.
Allen, R. G., Pereira, L. S., Raes, D., & Smith, M. (1998). *FAO Irrigation and Drainage Paper No. 56 - Crop Evapotranspiration. 56.*
Allen, Richard G., Tasumi, M., Morse, A., Trezza, R., Wright, J. L., Bastiaanssen, W., Kramber, W., Lorite, I., & Robison, C. W. (2007). Satellite-Based Energy Balance for Mapping Evapotranspiration with Internalized Calibration (METRIC)—Applications. *Journal of Irrigation and Drainage Engineering*, *133*(4), 395–406. https://doi.org/10.1061/(asce)0733-9437(2007)133:4(395)
Bassi, M. A., Lopez, M. A., Confalone, L., Gaudio, R. M., Lombardo, L., & Lauritano, D. (2020). Enhanced Reader.pdf. In *Nature* (Vol. 388, pp. 539–547).
Blatchford, M. L., Mannaerts, C. M., Njuki, S. M., Nouri, H., Zeng, Y., Pelgrum, H., Wonink, S., & Karimi, P. (2020). Evaluation of WaPOR V2 evapotranspiration products across Africa. *Hydrological Processes*, *34*(15), 3200–3221. https://doi.org/10.1002/hyp.13791
Brenner, C., Zeeman, M., Bernhardt, M., & Schulz, K. (2018). Estimation of evapotranspiration of temperate grassland based on high-resolution thermal and visible range imagery from unmanned aerial systems. *International Journal of Remote Sensing*, *39*(15–16), 5141–5174. https://doi.org/10.1080/01431161.2018.1471550
Bucagu, C. (2013). Tailoring agroforestry technologies to the diversity of Rwandan smallholder agriculture. In *Tailoring agroforestry technologies to the diversity of Rwandan smallholder agriculture.* http://search.ebscohost.com/login.aspx?direct=true&db=lah&AN=20133366587&site=ehost-live
Carlson, T. (2007). An overview of the "triangle method" for estimating surface evapotranspiration and soil moisture from satellite imagery. *Sensors*, *7*(8), 1612–1629. https://doi.org/10.3390/s7081612
Carlson, T. N., & Petropoulos, G. P. (2019). A new method for estimating of evapotranspiration and surface soil moisture from optical and thermal infrared measurements: the simplified triangle. *International Journal of Remote Sensing*, *40*(20), 7716–7729. https://doi.org/10.1080/01431161.2019.1601288
Chauhan, N. S., Miller, S., & Ardanuy, P. (2003). Spaceborne soil moisture estimation at high resolution: A microwave-optical/IR synergistic approach. *International Journal of Remote Sensing*, *24*(22), 4599–4622. https://doi.org/10.1080/0143116031000156837
Ellsäßer, F., Stiegler, C., Röll, A., June, T., Knohl, A., & Hölscher, D. (2020). Predicting evapotranspiration from drone-based thermography – a method comparison in a tropical oil palm plantation. *Biogeosciences Discussions*, 1–37. https://doi.org/10.5194/bg-2020-159
European Space Agency. (2017). *SMOS Data Products. November.* http://bec.icm.csic.es/land-datasets
FAO. (2016a). Coping with Water Scarcity in Agriculture: a Global Framework for Action in a Changing Climate. In *FAO* (pp. 1–12). http://www.fao.org/documents/card/en/c/8dd680fd-70d3-4725-8d9f-30f9a02455a0/?utm_content=bufferf93b2&utm_medium=social&utm_source=twitter.com&utm_campaign=buffer
FAO. (2016b). Coping with Water Scarcity in Agriculture. *Food and Agriculture Organization of the United Nations*, 1–12. http://www.fao.org/documents/card/en/c/8dd680fd-70d3-4725-8d9f-30f9a02455a0/?utm_content=bufferf93b2&utm_medium=social&utm_source=twitter.com&utm_campaign=buffer
FAO. (2017a). The Future of Food and Agriculture. In *Food and Agriculture Organization of the United Nations* (Issue November). http://www.fao.org/3/i6583e/i6583e.pdf
FAO. (2017b). Water for Sustainable Food and Agriculture Water for Sustainable Food and Agriculture. In *A report produced for the G20 Presidency of Germany*. www.fao.org/publications
FAO. (2018a). WaPOR Database Methodology: Level 2 Data Using Remote Sensing in Support of Solutions To Reduce Agricultural Water Productivity Gaps. In *Food and Agriculture Organization of the United Nations (FAO)* (Issue December). FAO. http://www.fao.org/3/i7315en/i7315en.pdf
FAO. (2018b). WaPOR Database Methodology: Level 2 Data Using Remote Sensing in Support of Solutions To Reduce Agricultural Water Productivity Gaps. In *Food and Agriculture Organization of the*

United Nations (FAO) (Issue December). http://www.fao.org/3/i7315en/i7315en.pdf
FAO. (2020a). WaPOR database methodology. In *WaPOR database methodology*. https://doi.org/10.4060/ca9894en
FAO. (2020b). WaPOR database methodology. In *WaPOR database methodology* (Issue April). https://doi.org/10.4060/ca9894en
FAO and IHE Delft. (2019). *WaPOR quality assessment.Technical report on the data quality of the WaPOR FAO database*. IHE Delft.
Fenta Mekonnen, D. (2009). *Satellite Remote Sensing for Soil Moisture Estimation: Gumara Catchment, Ethiopia*.
Foster, T., Brozović, N., Butler, A. P., Neale, C. M. U., Raes, D., Steduto, P., Fereres, E., & Hsiao, T. C. (2017). AquaCrop-OS: An open source version of FAO's crop water productivity model. *Agricultural Water Management*, *181*, 18–22. https://doi.org/10.1016/j.agwat.2016.11.015
Government of Rwanda (NISR, M. o. E. (2019). Rwanda Natural Capital Accounts - Ecosystems. In *NISR,Ministry of Environment* (Issue November). www.moe.gov.rw
Henninger, S. M. (2013). Does the global warming modify the local Rwandan climate? *Natural Science*, *05*(01), 124–129. https://doi.org/10.4236/ns.2013.51a019
Jin, X., Yang, G., Li, Z., Xu, X., Wang, J., & Lan, Y. (2018). Estimation of water productivity in winter wheat using the AquaCrop model with field hyperspectral data. *Precision Agriculture*, *19*(1), 1–17. https://doi.org/10.1007/s11119-016-9469-2
Jing, P., & Li, D. (2014). *Atmospheric and Oceanic Science Letters The Soil Moisture and Net Primary Production Affected by CO 2 and Climate Change Using a Coupled Model The Soil Moisture and Net Primary Production Affected by CO 2 and Climate Change Using a Coupled Model*. *7*(4), 269–274. https://doi.org/10.3878/j.issn.1674-2834.13.0100
Macpherson, D. (2013). *Report on an aerial census of Akagera national park, Rwanda - August 2013*. *October*, 1–45. https://www.african-parks.org/sites/default/files/uploads/newsroom_file_upload/2017-05/Akagera_National_Park_Rwanda_Aerial_Census_-_August_2013_%281%29.pdf
Mali, S. S. (2016). Basic Concepts of Water Productivity. *Approaches to Improve Agricultural Water Productivity*, *July*.
Mekuria, E. F. (2012). *SPATIAL AND TEMPORAL ANALYSIS OF RECENT DROUGHT Case of Somali regional state of Ethiopia*. 1–79.
Mugabowindekwe, M., & Rwanyiziri, G. (2020). Comparative Assessment of Homogeneity Differences in Multi-Temporal NDVI Strata and the Currently Used Agricultural Area Frames in Rwanda. *South African Journal of Geomatics*, *9*(1), 89–107. https://doi.org/10.4314/sajg.v9i1.7
Nichols, S. (2011). Review and evaluation of remote sensing methods for soil-moisture estimation. *Journal of Photonics for Energy*, *May*, 028001. https://doi.org/10.1117/1.3534910
Pierdicca, N., Pulvirenti, L., Fascetti, F., Crapolicchio, R., & Talone, M. (2013). Analysis of two years of ASCAT- and SMOS-derived soil moisture estimates over Europe and North Africa. *European Journal of Remote Sensing*, *46*(1), 759–773. https://doi.org/10.5721/EuJRS20134645
Price, J. C. (1990). U sing Spatial Context in Satellite Data to Infer Regional Scale Evapotranspiration. *IEEE Transactions on Geoscience and Remote Sensing*, *28*(5), 940–948. https://doi.org/10.1109/36.58983
Prospects, W. P. (2020). *Population Facts*. *2019*, 1–4.
Querner, E., Herder, C., Fissahaye, D., & Froebrich, J. (2014). *Modelling crop production in water-scarce basins with SWAT ; case studies of the Limpopo River basin and in Ethiopia* (Issue 265471). www.wageningenUR.nl/en/alterra.
Rahmati, M., Oskouei, M. M., Neyshabouri, M. R., Walker, J. P., Fakherifard, A., Ahmadi, A., & Mousavi, S. B. (2015a). Soil moisture derivation using triangle method in the lighvan watershed, north western Iran. *Journal of Soil Science and Plant Nutrition*, *15*(1), 167–178. https://doi.org/10.4067/S0718-95162015005000014
Rahmati, M., Oskouei, M. M., Neyshabouri, M. R., Walker, J. P., Fakherifard, A., Ahmadi, A., & Mousavi, S. B. (2015b). Soil moisture derivation using triangle method in the lighvan watershed, north western Iran. *Journal of Soil Science and Plant Nutrition*, *15*(1), 167–178. https://doi.org/10.4067/S0718-95162015005000014
RDB. (2019). *AKAGERA NATIONAL PARK RWANDA Akagera totals 1,122km 2*. www.twitter.com/AfricanParks
Saadi, S. (2018). *Spatial estimation of actual evapotranspiration and irrigation volumes using water and energy balance models forced by optical remote sensing data (VIS / NIR / TIR) Sameh Saadi To cite this version : HAL Id : tel-*

01720420. https://tel.archives-ouvertes.fr/tel-01720420
Sánchez, N., Martínez-Fernánadez, J., Scaini, A., & Pérez-Gutierrez, C. (2012). Validation of the SMOS L2 soil moisture data in the REMEDHUS network (Spain). *IEEE Transactions on Geoscience and Remote Sensing*, *50*(5 PART 1), 1602–1611. https://doi.org/10.1109/TGRS.2012.2186971
Sayler, K., & Zanter, K. (2020). Landsat 8 Level 2 Science Product (L2SP) Guide. *Nasa*, *2*(May). https://prd-wret.s3.us-west-2.amazonaws.com/assets/palladium/production/atoms/files/LSDS-1619_Landsat8-C2-L2-ScienceProductGuide-v2.pdf
Sayler, Kristi. (2020). *Landsat 8 Collection 2 (C2) Level 2 Science Product (L2SP) Guide*.
Silva-Fuzzo, D. F., & Rocha, J. V. (2016). Simplified triangle method for estimating evaporative fraction over soybean crops. *Journal of Applied Remote Sensing*, *10*(4), 046027. https://doi.org/10.1117/1.jrs.10.046027
Silva, V. de P. R. da, e Silva, R. A., Maciel, G. F., Braga, C. C., da Silva Júnior, J. L. C., de Souza, E. P., Almeida, R. S. R., Silva, M. T., & de Holanda, R. M. (2018). Calibração e validação do modelo AquaCrop para a cultura de soja cultivada mediante diferentes níveis de irrigação na região de Matopiba, Brasil. *Ciencia Rural*, *48*(1). https://doi.org/10.1590/0103-8478cr20161118
Souza, A. G. S. S., Neto, A. R., Rossato, L., Alvalá, R. C. S., & Souza, L. L. (2018). Use of SMOS L3 soil moisture data: Validation and drought assessment for Pernambuco State, Northeast Brazil. *Remote Sensing*, *10*(8), 1–19. https://doi.org/10.3390/RS10081314
Timmermans, W. J., Kustas, W. P., & Andreu, A. (2015). Utility of an Automated Thermal-Based Approach for Monitoring Evapotranspiration. *Acta Geophysica*, *63*(6), 1571–1608. https://doi.org/10.1515/acgeo-2015-0016
Vaghefi, S. A., Abbaspour, K. C., Faramarzi, M., Srinivasan, R., & Arnold, J. G. (2017). Modeling crop water productivity using a coupled SWAT-MODSIM model. *Water (Switzerland)*, *9*(3), 157. https://doi.org/10.3390/w9030157
Wang, L., Qu, J. J., Zhang, S., Hao, X., & Dasgupta, S. (2007). Soil moisture estimation using MODIS and ground measurements in Eastern China. *International Journal of Remote Sensing*, *28*(6), 1413–1418. https://doi.org/10.1080/01431160601075525
World Bank Group. (2021). *World Bank Climate Change Knowledge Portal - Malta*. Climate Change Knowlwdge Portal. https://climateknowledgeportal.worldbank.org/country/rwanda/climate-data-historical
Xia, T., Kustas, W. P., Anderson, M. C., Alfieri, J. G., Gao, F., McKee, L., Prueger, J. H., Geli, H. M. E., Neale, C. M. U., Sanchez, L., Alsina, M. M., & Wang, Z. (2016). Mapping evapotranspiration with high-resolution aircraft imagery over vineyards using one-and two-source modeling schemes. *Hydrology and Earth System Sciences*, *20*(4), 1523–1545. https://doi.org/10.5194/hess-20-1523-2016
Zotarelli, L., Dukes, M. D., Romero, C. C., Migliaccio, K. W., & Kelly, T. (2020). *Step by Step Calculation of the Penman-Monteith Evapotranspiration (FAO-56 Method) 1*. 1–10.
Zotarelli, L., Dukes, M. D., Romero, C. C., Migliaccio, K. W., & Morgan, K. T. (2014). Step by Step Calculation of the Penman-Monteith Evapotranspiration (FAO-56 Method). AE459. *Institute of Food and Agricultural Sciences. University of Florida*, 1–14. http%22//edis.ifas.ufl.edu/ae459

APPENDIX 1

Example of ILWIS script used to derive ETa using DATTUTDUT model

%1 -%4 indicate 4 parameters
%1: LSTmin (the 0.5% of coldest pixels)
%2: DOY
%3: LSTmax
%4: UTC

// begin comment
lati%2{dom=VALUE.dom;vr=180.0000:180.0000:0.00001}:=iff(LST%2,crdy(transform(mapcrd(LST%),latlon)),0)
long%2{dom=VALUE.dom;vr=180.0000:180.0000:0.00001}:=iff(LST%2,crdx(transform(mapcrd(LST%2),latlon)),0)**// end comment**

om%2ega{dom=VALUE.dom;vr=-180.00000:180.00000:0.00001}:=(12-((%4)+long%2/15+et(da(%2))/60))*15
co%2zen{dom=VALUE.dom;vr=-1.0000:1.0000:0.00001}:=sin(de(da(%2))/57.29577951)*sin(lati%2/57.29577951)+cos(de(da(%2))/57.29577951)*cos(lati%2/57.29577951)*cos(om%2ega/57.29577951)
ir%2toa{dom=VALUE.dom;vr=-500000.0000:500000.0000:0.00001}:=1367*eo(da(%2))*co%2zen

// Calculation of the net radiation albedo map – instantaneous
r%2n.mpr{dom=VALUE.dom;vr=-5000.00000:5000.00000:0.00001}:= 0.85*0.75*ir%2toa+0.8*5.6697E-8*(%1)^(4)-0.95*5.6697E-8*(LST%2)^(4)
r%2n.mpr{dom=VALUE.dom;vr=-5000.00000:5000.00000:0.00001}:= (1-(0.05+(LST%2-%1)/(%3-%1)*0.2))*0.7*ir%2toa+0.8*5.6697E-8*(%1)^(4)-1.0*5.6697E-8*(LST%2)^(4)

// Calculation of the soil heat flux map – instantaneous
g%2s.mpr{dom=VALUE.dom;vr=-5000.00000:5000.00000:0.00001}:= (0.05+(LST%2-%1)/(%3-%1)*0.4)*r%2n

// Calculation of turbulent fluxes
h%2:=iff(LST%2<%1,0,iff(LST%2>%3,r%2n-g%2s,(r%2n-g%2s)*(LST%2-(%1))/(%3-%1)))
le%2:=r%2n-g%2s-h%2

// Daily values:
lambda%2.mpr{dom=VALUE.dom;vr=-1.00000:1.00000:0.0000}:=le%2/(le%2+h%2)
// Calculation of daily totals (assuming n/N equal to 1):
om%2egasr.mpr{dom=VALUE.dom;vr=-180.00000:180.00000:0.00001}:=acos(-1*tan(lati%2/57.29577951)*tan(de(da(%2))/57.29577951))
ir%2toaday.mpr{dom=VALUE.dom;vr=-5000.00000:5000.00000:0.00001}:=24/3.141592*1367*0.0036*eo(da(%2))*cos(lati%2/57.29577951)*cos(de(da(%2))/57.29577951)*(sin(om%2egasr)-om%2egasr*cos(om%2egasr))

APPENDIX 1

qn%2day.mpr{dom=VALUE.dom;vr=-5000.00000:5000.00000:0.00001}:=(0.25+0.5*1)*(1-1.1*(0.05+(LST%2-%1)/(%3-%1)*0.2))*ir%2toaday-110*(0.7)/11.5741
qn%2daydtd.mpr{dom=VALUE.dom;vr=-5000.00000:5000.00000:0.00001}:=(0.25+0.5*1)*(1-1.1*ro%2sur)*ir%2toaday-110*(%3/ir%2toa)/11.5741
et%2day.mpr{dom=VALUE.dom;vr=-5.00000:50.00000:0.001}:=lambda%2*qn%2day/2.47

APPENDIX 2

Example of a python script used to retrieve 2m temperature from ERA5-Land

```
import cdstoolbox as ct
@ct.application(title='Retrieve Data')
@ct.output.download()
def retrieve_sample_data():
    """
Application main steps:
    - retrieve a variable from CDS Catalogue
    - produce a link to download it.
    """
   # Time range
    data = ct.catalogue.retrieve(
        'reanalysis-era5-land',
        {   'variable': '2m_temperature',
            'product_type': 'reanalysis',
            'year':  ['2019'],
                'month': [  '06', ],
            'day': [  '21', ],
            'time': [
                '00:00', '01:00',    '02:00', '03:00',   '04:00', '05:00',
                '06:00', '07:00',    '08:00', '09:00',   '10:00', '11:00',
                '12:00', '13:00',    '14:00', '15:00',   '16:00', '17:00',
                '18:00', '19:00',    '20:00', '21:00',   '22:00', '23:00', ],
 }   )
   return data
```

Example of a python script used to retrieve dew temperature from ERA5-Land

```
import cdstoolbox as ct
@ct.application(title='Retrieve Data')
@ct.output.download()
def retrieve_sample_data():
    """
Application main steps:
    - retrieve a variable from CDS Catalogue
    - produce a link to download it.
    """
   # Time range
    data = ct.catalogue.retrieve(
        'reanalysis-era5-land',
        {   'variable': 'dew_temperature',
            'product_type': 'reanalysis',
            'year':  ['2019'],
```

```
  'month': [  '06', ],
          'day': [  '21', ],
          'time': [
              '00:00', '01:00',    '02:00', '03:00',   '04:00', '05:00',
              '06:00', '07:00',    '08:00', '09:00',   '10:00', '11:00',
              '12:00', '13:00',    '14:00', '15:00',   '16:00', '17:00',
              '18:00', '19:00',    '20:00', '21:00',   '22:00', '23:00', ],
}   )
  return data
```

Example of a python script used to retrieve 10m u- component of wind from ERA5-Land

```
import cdstoolbox as ct
@ct.application(title='Retrieve Data')
@ct.output.download()
def retrieve_sample_data():
    """
Application main steps:
    - retrieve a variable from CDS Catalogue
    - produce a link to download it.
    """
  # Time range
   data = ct.catalogue.retrieve(
       'reanalysis-era5-land',
       {   'variable': '10m_u_component_of_wind',
          'product_type': 'reanalysis',
          'year':  ['2019'],
              'month': [  '06', ],
          'day': [  '21', ],
          'time': [
              '00:00', '01:00',    '02:00', '03:00',   '04:00', '05:00',
              '06:00', '07:00',    '08:00', '09:00',   '10:00', '11:00',
              '12:00', '13:00',    '14:00', '15:00',   '16:00', '17:00',
              '18:00', '19:00',    '20:00', '21:00',   '22:00', '23:00', ],
}   )
  return data
```

Example of a python script used to retrieve 10m v- component of wind from ERA5-Land

```
import cdstoolbox as ct
@ct.application(title='Retrieve Data')
```

APPENDIX 2

```
@ct.output.download()
def retrieve_sample_data():
    """
Application main steps:
    - retrieve a variable from CDS Catalogue
    - produce a link to download it.
    """
   # Time range
    data = ct.catalogue.retrieve(
        'reanalysis-era5-land',
        {   'variable': '10m_v_component_of_wind',
            'product_type': 'reanalysis',
            'year':  ['2019'],
                'month': [  '06', ],
            'day': [  '21', ],
            'time': [
                '00:00', '01:00',    '02:00', '03:00',   '04:00', '05:00',
                '06:00', '07:00',    '08:00', '09:00',   '10:00', '11:00',
                '12:00', '13:00',    '14:00', '15:00',   '16:00', '17:00',
                '18:00', '19:00',    '20:00', '21:00',   '22:00', '23:00', ],
 }   )
   return data
```